Analysis of the small viscosity and large reaction coefficient in the computation of the generalized Stokes problem by a novel stabilized finite element method

Huo-Yuan Duan[a], Po-Wen Hsieh[b], Roger C. E. Tan[c], Suh-Yuh Yang[d,*]

[a]*Collaborative Innovation Centre of Mathematics, School of Mathematics and Statistics, Wuhan University, Wuhan 430072, China*
[b]*Department of Applied Mathematics, Chung Yuan Christian University, Jhongli City, Taoyuan County 32023, Taiwan*
[c]*Department of Mathematics, National University of Singapore, 2 Science Drive 2, Singapore 117543, Singapore*
[d]*Department of Mathematics, National Central University, Jhongli City, Taoyuan County 32001, Taiwan*

Abstract

In this paper, we propose and analyze a novel stabilized finite element method (FEM) for the system of generalized Stokes equations arising from the time-discretization of transient Stokes problem. The system involves a small viscosity, which is proportional to the inverse of large Reynolds number, and a large reaction coefficient, which is the inverse of small time step. The proposed stabilized FEM employs the C^0 piecewise linear elements for both velocity field and pressure on the same mesh and uses the residuals of the momentum equation and the divergence-free equation to define the stabilization terms. The stabilization parameters are fixed and element-independent, without a comparison of the viscosity, the reaction coefficient and the mesh size. Using the finite element solution of an auxiliary boundary value problem as the interpolating function for velocity and the H^1-seminorm projection for pressure, instead of the usual nodal interpolants, we derive error estimates for the stabilized finite element approximations to velocity and pressure in the L^2 and H^1 norms and most importantly, we explicitly establish the dependence of error bounds on the viscosity, the reaction coefficient and the mesh size. Our analysis reveals that this stabilized FEM is particularly suitable for the generalized Stokes system with a small viscosity and a large reaction coefficient, which has never been achieved before in the error analysis of other stabilization methods in the literature. We then numerically confirm the effectiveness of the proposed stabilized FEM. Comparisons made with other existing stabilization methods show that the newly proposed method can attain better accuracy and stability.

Keywords: generalized Stokes problem, small viscosity, large reaction coefficient, stabilized finite element method, stabilization parameter

2000 MSC: 65N12, 65N15, 65N30, 76M10

1. Introduction

Let $\Omega \subset \boldsymbol{R}^2$ be a bounded open convex polygonal domain with boundary $\partial\Omega$. In this paper, we propose and analyze a novel stabilized finite element method (FEM) for solving the following system of generalized Stokes equations with no-slip boundary condition:

$$\left\{ \begin{array}{rcll} \sigma \boldsymbol{u} - \nu \Delta \boldsymbol{u} + \nabla p &=& \boldsymbol{f} & \text{in } \Omega, \\ \nabla \cdot \boldsymbol{u} &=& 0 & \text{in } \Omega, \\ \boldsymbol{u} &=& \boldsymbol{0} & \text{on } \partial\Omega, \end{array} \right. \tag{1}$$

*Corresponding author. Tel.: +886-3-4227151 extension 65130; fax: +886-3-4257379.
Email addresses: mathduanhuoyuan@yahoo.com (Huo-Yuan Duan), pwhsieh0209@gmail.com (Po-Wen Hsieh), scitance@nus.edu.sg (Roger C. E. Tan), syyang@math.ncu.edu.tw (Suh-Yuh Yang)

where $\boldsymbol{u} = (u_1, u_2)^\top$ is the velocity field and p is the pressure; $0 < \nu \leq 1$ is the kinematic viscosity which is proportional to the inverse of Reynolds number Re; $\sigma \geq 1$ is the reaction coefficient; and $\boldsymbol{f} = (f_1, f_2)^\top \in (L^2(\Omega))^2$ is a given source-like function. In principle, one of the parameters σ and ν in the generalized Stokes system (1) can be normalized as unity if we replace the velocity field with either $\sigma\boldsymbol{u}$ or $\nu\boldsymbol{u}$. However, in order to explicitly display the parameters σ and ν in our finite element error estimates and to serve as a base for the future study of more advanced incompressible Navier-Stokes system which contains an additional nonlinear velocity convection term and therefore the normalization cannot be applied, in this paper we keep the generalized Stokes system in its primitive form (1).

Typically, the generalized Stokes system (1) may arise from the time discretization of transient Stokes problem, where the reaction coefficient σ is inversely proportional to the time step δt. For problems involving chemical reactions, a small time step, namely a large σ, is needed in order to account for the stiffness due to the fast reaction [1, 2, 3]. In fact, the common finite element approach to the time-dependent PDEs is based on the so-called method of lines. That is, a semi-discrete formulation is formed by first approximating the spatial dependence using a certain finite element method, and the resulting ODE system is then discretized by applying implicit finite differences in time domain, such as the first-order backward Euler scheme or the second-order Crank-Nicolson scheme, to obtain a fully discrete problem [4, 5]. One can find that at each time level with an implicit time discretization, the resulting fully discrete problem is analogue to the finite element method applied directly to the generalized Stokes system (1).

The usual mixed FEM for solving problem (1) is to discretize the following weak form by employing a pair of finite element spaces $(\mathcal{V}_h, \mathcal{Q}_h)$ for the approximations of $\boldsymbol{u}$ and p: *Find* $(\boldsymbol{u}, p) \in (H_0^1(\Omega))^2 \times L_0^2(\Omega)$ *such that*

$$\sigma(\boldsymbol{u}, \boldsymbol{v})_0 + \nu(\nabla\boldsymbol{u}, \nabla\boldsymbol{v})_0 - (p, \nabla\cdot\boldsymbol{v})_0 + \gamma(\nabla\cdot\boldsymbol{u}, q)_0 = (\boldsymbol{f}, \boldsymbol{v})_0, \tag{2}$$

for all $(\boldsymbol{v}, q) \in (H_0^1(\Omega))^2 \times L_0^2(\Omega)$, where $\gamma = \pm 1$ correspond to a symmetric method and a non-symmetric method. However, it is now well known that the pair $(\mathcal{V}_h, \mathcal{Q}_h)$ must satisfy the so-called inf-sup condition if stable and optimally accurate approximations are desired; see [6, 7, 8, 9]. Unfortunately, this condition prevents the use of standard equal order C^0 interpolation spaces for velocity and pressure with respect to the same triangulation that are the most attractive from the viewpoint of implementation, or low order element pairs such as piecewise linear elements for velocity and piecewise constants for pressure.

In order to circumvent the inf-sup condition, a class of the so-called stabilized FEMs has been developed and intensively studied for almost thirty years, see, e.g., [10, 11, 12, 13, 14, 15, 16]. The stabilized FEMs are formed by adding to the discrete counterpart of the weak formulation (2) with the residuals of the partial differential equations. An example for the derivation of such a stabilized FEM is based on the bubble condensation procedure (cf. [17, 18]). This approach adopts a mixed finite element formulation but enriches the C^0 piecewise P_1 (or Q_1) elements for velocity field $\boldsymbol{u}$ with suitable bubble functions and then give an expression of the bubble part of velocity in terms of its linear part, pressure p and source function $\boldsymbol{f}$. Such a bubble condensation procedure eventually leads to a stabilization method. A common feature for all stabilization methods is that some mesh-dependent stabilization parameters are involved with. The stabilization parameters play key roles in the method, not only enhancing the numerical stability

but also improving the accuracy in the finite element solutions. Nowadays, it is very popular to apply finite element stabilization techniques to produce better accuracy and stability in the finite element solution of convection-dominated convection-diffusion problems [19, 20, 21, 22, 23, 24, 25, 26, 27, 28, 29], or to circumvent the inf-sup condition in solving saddle-point type problems such as the incompressible Stokes equations [1, 17, 30, 31, 32]; see also [2] and many references cited therein. However, it has been observed that the pressure instabilities may be caused in time step of the transient problems, as the time step $\delta t \approx 1/\sigma$ becomes small compared to the spatial grid size h; see [1, 2, 3]. Therefore, in recent years, it has attracted a great deal of attention on the theoretical and computational studies of small time-step instabilities when implicit, finite difference time integration is applied in combination with finite element stabilization in the spatial semi-discretization.

In this paper, we will propose and analyze a new stabilized FEM for problem (1) with a small viscosity ν and a large reaction coefficient σ. With novel stabilization parameters, we employ the C^0 piecewise P_1 (or Q_1) elements for both velocity field and pressure on the same mesh and use the residuals of the partial differential equations to define the stabilization terms. These additional stabilization terms include not only the term related to the momentum equation but also the divergence-free equation. Another feature, different from the stabilization methods, e.g., [17, 30], in the literature is that our stabilization parameters are fixed and element-independent, without the comparison among the viscosity ν, the reaction coefficient σ and the mesh size h. The third feature is that our error analysis is novel. We use the finite element solution of an auxiliary boundary value problem as the interpolating function for velocity and the H^1-seminorm projection [9] for pressure, instead of the usual nodal interpolants $\mathcal{I}_h\boldsymbol{u}$ and $\mathcal{I}_h p$. This novel technique enables us to show that the proposed stabilized FEM using C^0 piecewise equal-order finite elements, such as P_1-P_1 and Q_1-Q_1 elements, is particularly suitable for problem (1) with a small ν and a large σ.

We will derive error estimates in the L^2 and H^1 norms for the proposed stabilized FEM using the C^0 piecewise P_1-P_1 (or Q_1-Q_1) elements. Most importantly, we will explicitly establish the dependence of the error bounds on the parameters ν, σ and h. Roughly speaking, we prove that, leaving aside the term "$\|\boldsymbol{u}\|_2 + \|p\|_1$" of regularity norm of the exact solution, the H^1-norm error bound of the velocity is inversely proportional to the square root of the reaction coefficient σ, the L^2-norm error bound behaves like the multiplication of the H^1-norm error bound by the mesh size h, and that the L^2-norm error bound of the pressure is in the same order of $h + \sqrt{\nu}$ if $\sigma h^2 \gg \nu$. Moreover, we will compare numerically the effectiveness of the newly proposed stabilized FEM with three existing stabilization methods in the literature, including the Barrenechea-Blasco stabilized FEM [30], the Barrenechea-Valentin stabilized FEM [17], and the Bochev-Gunzburger-Lehoucq stabilized FEM [1]. Through a series of numerical experiments, we find that in addition to offer rather sharp error estimates, the proposed stabilized FEM can achieve better accuracy and stability when compared with the Barrenechea-Blasco method and the Bochev-Gunzburger-Lehoucq method, while it is comparable with the Barrenechea-Valentin method when $\sigma h^2 \gg \nu$ and $0 < \nu \ll 1$.

We remark that the div-div stabilization term related to the divergence-free equation in the finite element formulation was first introduced in [33]; see also, e.g., [32, 34, 35]. It has been proved in [36] that the div-div stabilization term results in better error bounds of finite element solutions for the generalized Stokes equations (1). However, in

that method, the finite element pair $(\mathcal{V}_h, \mathcal{Q}_h)$ has to satisfy the inf-sup condition, the analysis focuses on the small reaction coefficient $\sigma \in [0, 1]$, and the error bounds for the velocity are measured in the viscosity $\sqrt{\nu}$-weighted H^1-seminorm. Therefore, the use of equal order C^0 finite element spaces for velocity and pressure is prevented and the poor convergence may be caused by small viscosity ν and large reaction coefficient σ. In contrast, in this paper, the newly proposed stabilized FEM is an unusual stabilization method inspired by the works of Franca-Farhat [22] and Barrenechea-Valentin [17]. It employs the C^0 piecewise equal-order finite elements aiming at dealing with small viscosity and large reaction. Our analysis reveals that the viscosity ν and the reaction constant σ respectively act in the numerator position and the denominator position in the error estimates of velocity and pressure in standard norms without any weights; see Theorem 5 and Theorem 6 in Section 3. In other words, up to the regularity norm "$\|\boldsymbol{u}\|_2 + \|p\|_1$" of the exact solution, the proposed method is particularly suitable for the generalized Stokes system (1) with a small viscosity ν and a large reaction coefficient σ. Recently, it has also been shown in [37] that the finite element formulation including the div-div stabilization term is more effective for convection-dominated problems, such as the Oseen equations with a small viscosity.

In summary, the main goal of this paper are three aspects. The first is to develop a new unusual stabilization method in order to obtain better error bounds. The second is to provide a new analysis to prove the robustness of the unusual stabilization methods with respect to the small viscosity ν and the large reaction σ. The third is to provide numerical experiments to further demonstrate the robustness of the unusual type stabilization methods, including the proposed stabilized FEM and the Barrenechea-Valentin stabilized FEM, for the generalized Stokes equations with small viscosity and large reaction. These three aspects will be successfully realized in this paper.

The remainder of this paper is organized as follows. In Section 2, we introduce the new stabilized FEM and present three existing stabilized FEMs in the literature. In Section 3, error estimates of the newly proposed method are derived. The dependence of error bounds on the parameters ν, σ and h are explicitly established. In Section 4, several numerical examples are presented, including an example on the unstructured meshes and the time-dependent lid-driven cavity problem. Finally, in Section 5, summary and conclusions are given.

2. The new stabilized finite element method

We use the standard notation and definitions for the Sobolev spaces $H^m(\Omega)$ for nonnegative integers m (cf. [7, 9, 38, 39]). The associated inner product and norm are denoted by $(\cdot,\cdot)_m$ and $\|\cdot\|_m$, respectively. As usual, we define

$$\begin{aligned} L_0^2(\Omega) &= \{q \in L^2(\Omega) : \int_\Omega q = 0\}, \\ H_0^1(\Omega) &= \{v \in H^1(\Omega) : \ v = 0 \text{ on } \partial\Omega\}. \end{aligned}$$

Let $\{\mathcal{T}_h\}_{0<h\le 1}$ be a family of triangulations of Ω. A triangulation $\mathcal{T}_h$ of Ω into elements K consisting of triangles (or quadrilaterals) is performed in the usual way; the intersection of any two elements is a vertex, or an edge or empty, and $\overline{\Omega} = \cup_{K\in\mathcal{T}_h} K$. For each triangulation the subscript $h \in (0, 1]$ refers to the level of refinement of the triangulation. In particular, the mesh size parameter h is defined as $h = \max\{h_K : K \in \mathcal{T}_h\}$, where h_K denotes the diameter of element

K. We always assume that the family $\{\mathcal{T}_h\}_{0<h\leq 1}$ of triangulations is shape regular [6, 7, 38, 39]. As usual, $(\cdot,\cdot)_{m,K}$ and $\|\cdot\|_{m,K}$ denote the associated inner product and norm in $H^m(K)$, respectively, where K is a given element in $\mathcal{T}_h$.

Define the finite element space $\mathcal{V}_h = V_1 \times V_1$ for velocity $\boldsymbol{u}$, where $V_1 \subseteq H_0^1(\Omega)$ denotes the space of C^0 piecewise linear (or bilinear) finite elements over the triangulation $\mathcal{T}_h$. The standard interpolation theory [7, 38] ensures that if $\boldsymbol{u} \in (H^2(\Omega) \cap H_0^1(\Omega))^2$, then there exists an interpolant $\mathcal{I}_h\boldsymbol{u} \in \mathcal{V}_h$ such that

$$\|\boldsymbol{u} - \mathcal{I}_h\boldsymbol{u}\|_{s,K} \leq Ch_K^{2-s}\|\boldsymbol{u}\|_{2,K} \quad \forall\ 0 \leq s \leq 2,\ \forall\ K \in \mathcal{T}_h, \tag{3}$$

where C is a positive constant independent of K and h_K. Also, we define the C^0 piecewise linear (or bilinear) finite element space $Q_h \subseteq H^1(\Omega) \cap L_0^2(\Omega)$ for pressure p with the interpolation property: if $p \in H^2(\Omega) \cap L_0^2(\Omega)$, then there exists an interpolation $\mathcal{I}_h p \in Q_h$ such that

$$\|p - \mathcal{I}_h p\|_{s,K} \leq Ch_K^{2-s}\|p\|_{2,K} \quad \forall\ 0 \leq s \leq 2,\ \forall\ K \in \mathcal{T}_h. \tag{4}$$

We remark that in this paper we use C to denote a generic positive constant, possibly different at different occurrences, which is always independent of h and other parameters introduced.

Since the pair of finite element spaces $(\mathcal{V}_h, Q_h)$ does not verify the inf-sup condition, the corresponding discrete counterpart of the weak formulation (2) is generally unstable. Next, we are going to design a stabilization method for solving the generalized Stoke system (1). In what follows, for retaining the property of symmetry of the associated bilinear form, we only consider the case of $\gamma = -1$ in the weak form (2). We propose the following new stabilized FEM for the generalized Stokes system (1): *Find* $(\boldsymbol{u}_h, p_h) \in \mathcal{V}_h \times Q_h$ *such that*

$$B((\boldsymbol{u}_h, p_h), (\boldsymbol{v}_h, q_h)) = L((\boldsymbol{v}_h, q_h)) \quad \forall\ (\boldsymbol{v}_h, q_h) \in \mathcal{V}_h \times Q_h, \tag{5}$$

where the bilinear form $B(\cdot,\cdot)$ and the linear form $L(\cdot)$ are, respectively, defined as follows:

$$\begin{aligned} B((\boldsymbol{u}_h, p_h), (\boldsymbol{v}_h, q_h)) &= \sigma(\boldsymbol{u}_h, \boldsymbol{v}_h)_0 + \nu(\nabla\boldsymbol{u}_h, \nabla\boldsymbol{v}_h)_0 - (p_h, \nabla\cdot\boldsymbol{v}_h)_0 - (\nabla\cdot\boldsymbol{u}_h, q_h)_0 \\ &\quad - \sum_{K\in\mathcal{T}_h} \frac{h^2}{\sigma h^2 + 12\nu}(\sigma\boldsymbol{u}_h - \nu\Delta\boldsymbol{u}_h + \nabla p_h, \sigma\boldsymbol{v}_h - \nu\Delta\boldsymbol{v}_h + \nabla q_h)_{0,K} \\ &\quad + \sum_{K\in\mathcal{T}_h} \frac{12\nu}{\sigma h^2 + 12\nu}(\nabla\cdot\boldsymbol{u}_h, \nabla\cdot\boldsymbol{v}_h)_{0,K}, \end{aligned} \tag{6}$$

$$L((\boldsymbol{v}_h, q_h)) = (\boldsymbol{f}, \boldsymbol{v}_h)_0 - \sum_{K\in\mathcal{T}_h} \frac{h^2}{\sigma h^2 + 12\nu}(\boldsymbol{f}, \sigma\boldsymbol{v}_h - \nu\Delta\boldsymbol{v}_h + \nabla q_h)_{0,K}. \tag{7}$$

Note that in (6) and (7), we have $\Delta\boldsymbol{v}_h|_K = \boldsymbol{0}$ for all $K \in \mathcal{T}_h$ and $\boldsymbol{v}_h \in \mathcal{V}_h$. However, we still retain the terms therein for the clarity of presentation.

Here we remark that the stabilization terms in (6) include not only the term related to the momentum equation but also the continuity equation. This is quite different from the stabilization methods given in [1, 17, 30]; see also (13), (17) and (21) below. Furthermore, the test function in the momentum stabilization includes the reaction term $\sigma\boldsymbol{v}_h$ which is different again from that of [1, 30]. Secondly, the stabilization parameters $h^2/(\sigma h^2 + 12\nu)$ and $12\nu/(\sigma h^2 + 12\nu)$ in (6) are fixed and element-independent, without the comparison among ν, σ and h.

We next define the induced energy norm denoted by $\|\cdot\|_h$ on $\mathcal{V}_h \times \mathcal{Q}_h$, which is related to the bilinear form $B(\cdot,\cdot)$ introduced in (6),

$$\|(\boldsymbol{v}_h, q_h)\|_h^2 = \nu\|\nabla \boldsymbol{v}_h\|_0^2 + \frac{12\sigma\nu}{\sigma h^2 + 12\nu}\|\boldsymbol{v}_h\|_0^2 + \frac{h^2}{\sigma h^2 + 12\nu}\|\nabla q_h\|_0^2 + \frac{12\nu}{\sigma h^2 + 12\nu}\|\nabla \cdot \boldsymbol{v}_h\|_0^2. \tag{8}$$

Since $\int_\Omega q_h = 0$ for all $q_h \in \mathcal{Q}_h$, one can easily verify that $\|\cdot\|_h$ is indeed a norm on $\mathcal{V}_h \times \mathcal{Q}_h$. With this energy norm, we immediately have the following estimates of the continuous bilinear form $B(\cdot,\cdot)$ on $(\mathcal{V}_h \times \mathcal{Q}_h) \times (\mathcal{V}_h \times \mathcal{Q}_h)$:

Lemma 1. *The bilinear form $B(\cdot,\cdot)$ is weakly coercive on $(\mathcal{V}_h \times \mathcal{Q}_h) \times (\mathcal{V}_h \times \mathcal{Q}_h)$, that is,*

$$\inf_{\mathbf{0}\neq(\boldsymbol{v}_h,q_h)\in\mathcal{V}_h\times\mathcal{Q}_h} \sup_{\mathbf{0}\neq(\boldsymbol{\chi}_h,\varphi_h)\in\mathcal{V}_h\times\mathcal{Q}_h} \frac{B((\boldsymbol{v}_h,q_h),(\boldsymbol{\chi}_h,\varphi_h))}{\|(\boldsymbol{v}_h,q_h)\|_h\|(\boldsymbol{\chi}_h,\varphi_h)\|_h} \geq 1, \tag{9}$$

$$\inf_{\mathbf{0}\neq(\boldsymbol{\chi}_h,\varphi_h)\in\mathcal{V}_h\times\mathcal{Q}_h} \sup_{\mathbf{0}\neq(\boldsymbol{v}_h,q_h)\in\mathcal{V}_h\times\mathcal{Q}_h} \frac{B((\boldsymbol{v}_h,q_h),(\boldsymbol{\chi}_h,\varphi_h))}{\|(\boldsymbol{v}_h,q_h)\|_h\|(\boldsymbol{\chi}_h,\varphi_h)\|_h} \geq 1. \tag{10}$$

Proof. Given $(\boldsymbol{v}_h, q_h) \in \mathcal{V}_h \times \mathcal{Q}_h$, we have from (6) that

$$\begin{aligned} B((\boldsymbol{v}_h,q_h),(\boldsymbol{v}_h,-q_h)) &= \sigma\|\boldsymbol{v}_h\|_0^2 + \nu\|\nabla\boldsymbol{v}_h\|_0^2 - \frac{h^2}{\sigma h^2+12\nu}(\sigma\boldsymbol{v}_h + \nabla q_h, \sigma\boldsymbol{v}_h - \nabla q_h)_0 + \frac{12\nu}{\sigma h^2+12\nu}\|\nabla\cdot\boldsymbol{v}_h\|_0^2 \\ &= \nu\|\nabla\boldsymbol{v}_h\|_0^2 + \frac{12\sigma\nu}{\sigma h^2+12\nu}\|\boldsymbol{v}_h\|_0^2 + \frac{h^2}{\sigma h^2+12\nu}\|\nabla q_h\|_0^2 + \frac{12\nu}{\sigma h^2+12\nu}\|\nabla\cdot\boldsymbol{v}_h\|_0^2 \\ &= \|(\boldsymbol{v}_h,q_h)\|_h^2, \end{aligned}$$

which combining with the fact $\|(\boldsymbol{v}_h,-q_h)\|_h = \|(\boldsymbol{v}_h,q_h)\|_h$ implies

$$\sup_{\mathbf{0}\neq(\boldsymbol{\chi}_h,\varphi_h)\in\mathcal{V}_h\times\mathcal{Q}_h} \frac{B((\boldsymbol{v}_h,q_h),(\boldsymbol{\chi}_h,\varphi_h))}{\|(\boldsymbol{\chi}_h,\varphi_h)\|_h} \geq \|(\boldsymbol{v}_h,q_h)\|_h.$$

It clearly leads to (9). The estimate (10) holds by the symmetry property of the bilinear form $B(\cdot,\cdot)$. □

Notice that the weak coercivity (9)-(10) of the bilinear form $B(\cdot,\cdot)$ ensures the unique solvability of the stabilized FEM (5); see, e.g., [6, 7, 8]. We also remark that the stabilized FEM (5) is a consistent formulation, since (5) is satisfied when the finite element solution $(\boldsymbol{u}_h, p_h)$ is replaced by the exact solution $(\boldsymbol{u}, p)$ of the generalized Stokes system (1). As a consequence, we have the following orthogonality property:

$$B((\boldsymbol{u},p) - (\boldsymbol{u}_h,p_h),(\boldsymbol{v}_h,q_h)) = 0 \quad \forall\ (\boldsymbol{v}_h,q_h) \in \mathcal{V}_h \times \mathcal{Q}_h. \tag{11}$$

In the rest of this section, we give a brief review of three existing stabilized FEMs in the literature which are particularly designed for the generalized Stokes system (1) with a large reaction coefficient σ.

- **The Barrenechea-Blasco stabilized FEM:** In [30], Barrenechea and Blasco developed the following stabilized FEM: *Find $(\boldsymbol{u}_h, p_h) \in \mathcal{V}_h \times \mathcal{Q}_h$ such that*

$$B_{\mathrm{BB}}((\boldsymbol{u}_h,p_h),(\boldsymbol{v}_h,q_h)) = L_{\mathrm{BB}}((\boldsymbol{v}_h,q_h)) \quad \forall\ (\boldsymbol{v}_h,q_h) \in \mathcal{V}_h \times \mathcal{Q}_h, \tag{12}$$

where the bilinear form $B_{\rm BB}(\cdot,\cdot)$ and the linear form $L_{\rm BB}(\cdot)$ are, respectively, defined as follows:

$$\begin{aligned} B_{\rm BB}((\boldsymbol{u}_h,p_h),(\boldsymbol{v}_h,q_h)) &= \sigma(\boldsymbol{u}_h,\boldsymbol{v}_h)_0+\nu(\nabla\boldsymbol{u}_h,\nabla\boldsymbol{v}_h)_0-(\nabla\cdot\boldsymbol{v}_h,p_h)_0+(\nabla\cdot\boldsymbol{u}_h,q_h)_0 \\ &\quad -\sum_{K\in\mathcal{T}_h}\tau_K(\sigma\boldsymbol{u}_h-\nu\Delta\boldsymbol{u}_h+\nabla p_h,-\nu\Delta\boldsymbol{v}_h-\nabla q_h)_{0,K}, \qquad (13) \\ L_{\rm BB}((\boldsymbol{v}_h,q_h)) &= (\boldsymbol{f},\boldsymbol{v}_h)_0-\sum_{K\in\mathcal{T}_h}\tau_K(\boldsymbol{f},-\nu\Delta\boldsymbol{v}_h-\nabla q_h)_{0,K}, \qquad (14) \end{aligned}$$

τ_K is an element-dependent stabilization parameter given by

$$\tau_K=\alpha\frac{h_K^2}{\nu} \qquad (15)$$

and α is a positive constant such that

$$\tau_K<\min\left\{\frac{8}{\nu},\frac{3}{4\sigma}\right\}\quad\text{and}\quad\alpha<\frac{1}{4C_{\rm inv}^2}.$$

Here $C_{\rm inv}>0$ is the constant in the local inverse inequality [30]:

$$\|\Delta v_h\|_{0,K}\le C_{\rm inv}h_K^{-1}\|\nabla v_h\|_{0,K}\quad\forall\ K\in\mathcal{T}_h,\ v_h\in V_1.$$

In practical computations, we can take $C_{\rm inv}$ being any positive constant since $\|\Delta v_h\|_{0,K}=0$ for $v_h\in V_1$.

- **The Barrenechea-Valentin stabilized FEM:** Inspired by the work of [22, 25], Barrenechea and Valentin [17] introduced the following unusual stabilized FEM: *Find* $(\boldsymbol{u}_h,p_h)\in\mathcal{V}_h\times\mathcal{Q}_h$ *such that*

$$B_{\rm BV}((\boldsymbol{u}_h,p_h),(\boldsymbol{v}_h,q_h))=L_{\rm BV}((\boldsymbol{v}_h,q_h))\quad\forall\ (\boldsymbol{v}_h,q_h)\in\mathcal{V}_h\times\mathcal{Q}_h, \qquad (16)$$

where the bilinear form $B_{\rm BV}(\cdot,\cdot)$ and the linear form $L_{\rm BV}(\cdot)$ are, respectively, defined as follows:

$$\begin{aligned} B_{\rm BV}((\boldsymbol{u}_h,p_h),(\boldsymbol{v}_h,q_h)) &= \sigma(\boldsymbol{u}_h,\boldsymbol{v}_h)_0+\nu(\nabla\boldsymbol{u}_h,\nabla\boldsymbol{v}_h)_0-(\nabla\cdot\boldsymbol{v}_h,p_h)_0+(\nabla\cdot\boldsymbol{u}_h,q_h)_0 \\ &\quad -\sum_{K\in\mathcal{T}_h}\tau_K(\sigma\boldsymbol{u}_h-\nu\Delta\boldsymbol{u}_h+\nabla p_h,\sigma\boldsymbol{v}_h-\nu\Delta\boldsymbol{v}_h-\nabla q_h)_{0,K}, \qquad (17) \\ L_{\rm BV}((\boldsymbol{v}_h,q_h)) &= (\boldsymbol{f},\boldsymbol{v}_h)_0-\sum_{K\in\mathcal{T}_h}\tau_K(\boldsymbol{f},\sigma\boldsymbol{v}_h-\nu\Delta\boldsymbol{v}_h-\nabla q_h)_{0,K}, \qquad (18) \end{aligned}$$

τ_K is an element-dependent stabilization parameter given by

$$\tau_K=\frac{h_K^2}{\sigma h_K^2\xi(\lambda_K)+(4\nu/m_1)} \qquad (19)$$

and

$$\begin{aligned} &\lambda_K=\frac{4\nu}{m_1\sigma h_K^2},\quad m_1=\min\{1/3,C_1\}, \\ &C_1h_K^2\|\Delta v_h\|_{0,K}^2\le\|\nabla v_h\|_{0,K}^2\quad\forall\ v_h\in V_1,\quad \xi(\lambda)=\max\{\lambda,1\}. \end{aligned}$$

In practical computations, we take $m_1=1/3$ since $\|\Delta v_h\|_{0,K}=0$ for $v_h\in V_1$. The "unusual" feature of this stabilization method is the subtraction of a term $\sum_{K\in\mathcal{T}_h}\tau_K(\sigma\boldsymbol{u}_h,\sigma\boldsymbol{v}_h)_{0,K}$ from $\sigma(\boldsymbol{u}_h,\boldsymbol{v}_h)_0$ of the standard mixed FEM for the generalized Stokes system (1).

- **The Bochev-Gunzburger-Lehoucq stabilized FEM:** In [1], the authors considered the following stabilized FEM: *Find* $(\boldsymbol{u}_h, p_h) \in \mathcal{V}_h \times Q_h$ *such that*

$$B_{\mathrm{BGL}}((\boldsymbol{u}_h, p_h), (\boldsymbol{v}_h, q_h)) = L_{\mathrm{BGL}}((\boldsymbol{v}_h, q_h)) \quad \forall\ (\boldsymbol{v}_h, q_h) \in \mathcal{V}_h \times Q_h, \tag{20}$$

where the bilinear form $B_{\mathrm{BGL}}(\cdot,\cdot)$ and the linear form $L_{\mathrm{BGL}}(\cdot)$ are, respectively, defined as follows:

$$\begin{aligned} B_{\mathrm{BGL}}((\boldsymbol{u}_h, p_h), (\boldsymbol{v}_h, q_h)) &= \sigma(\boldsymbol{u}_h, \boldsymbol{v}_h)_0 + \nu(\nabla \boldsymbol{u}_h, \nabla \boldsymbol{v}_h)_0 - (\nabla \cdot \boldsymbol{v}_h, p_h)_0 - (\nabla \cdot \boldsymbol{u}_h, q_h)_0 \\ &\quad - \sum_{K \in \mathcal{T}_h} \tau_K (\sigma \boldsymbol{u}_h - \nu \Delta \boldsymbol{u}_h + \nabla p_h, -\gamma \nu \Delta \boldsymbol{v}_h + \nabla q_h)_{0,K}, \end{aligned} \tag{21}$$

$$L_{\mathrm{BGL}}((\boldsymbol{v}_h, q_h)) = (\boldsymbol{f}, \boldsymbol{v}_h)_0 - \sum_{K \in \mathcal{T}_h} \tau_K (\boldsymbol{f}, -\gamma \nu \Delta \boldsymbol{v}_h + \nabla q_h)_{0,K}, \tag{22}$$

$\gamma = -1, 0, 1$ and τ_K is an element-dependent stabilization parameter given by

$$\tau_K = \delta h_K^2 \tag{23}$$

and $\delta > 0$ is a parameter independent of h_K that needs to be carefully chosen.

We conclude this section with the following two remarks.

Remark 1. The choice of the first stabilization parameter $h^2/(\sigma h^2 + 12\nu)$ in the newly proposed stabilized FEM (5) is inspired by our recent work [40] on the scalar reaction-convection-diffusion equation and the element stabilization parameter τ_K described in (19). One can verify that if $\sigma h_K^2 \gg \nu$, then the element stabilization parameter τ_K in (19) can be expressed as

$$\tau_K = \frac{h_K^2}{\sigma h_K^2 + 12\nu},$$

which amounts to the first stabilization parameter $h^2/(\sigma h^2 + 12\nu)$ in (6) provided $h_K \geq Ch$.

Remark 2. All the above three stabilization methods, (12), (16) and (20), produce a non-symmetric algebraic system. The Barrenechea-Valentin method (16) also can be converted into a symmetric one by simply replacing q_h in the right-hand sides of (17) and (18) with $-q_h$. Note that our stabilization method (5) is symmetrical.

3. Error estimates of the new stabilized finite element method

We now proceed to estimate the error of the finite element solution $(\boldsymbol{u}_h, p_h)$ of the newly proposed stabilized FEM (5). Let $\boldsymbol{g} \in (L^2(\Omega))^2$ be a given source function. Consider the following auxiliary boundary value problem:

$$\begin{cases} \sigma \boldsymbol{w} - \nu \Delta \boldsymbol{w} = \boldsymbol{g} & \text{in } \Omega, \\ \boldsymbol{w} = \boldsymbol{0} & \text{on } \partial\Omega. \end{cases} \tag{24}$$

The corresponding stabilized FEM on the space $\mathcal{V}_h$ is defined as follows:

$$\textit{Find } \boldsymbol{w}_h \in \mathcal{V}_h \textit{ such that } B_{\mathrm{aux}}(\boldsymbol{w}_h, \boldsymbol{v}_h) = L_{\mathrm{aux}}(\boldsymbol{v}_h) \quad \forall\ \boldsymbol{v}_h \in \mathcal{V}_h, \tag{25}$$

where the bilinear form $B_{\text{aux}}(\cdot,\cdot)$ and the linear form $L_{\text{aux}}(\cdot)$ are, respectively, given by

$$B_{\text{aux}}(\boldsymbol{w}_h, \boldsymbol{v}_h) = \sigma(\boldsymbol{w}_h, \boldsymbol{v}_h)_0 + \nu(\nabla \boldsymbol{w}_h, \nabla \boldsymbol{v}_h)_0 - \sum_{K\in\mathcal{T}_h} \frac{h^2}{\sigma h^2 + 12\nu}(\sigma \boldsymbol{w}_h - \nu\Delta \boldsymbol{w}_h, \sigma \boldsymbol{v}_h - \nu\Delta \boldsymbol{v}_h)_{0,K}, \tag{26}$$

$$L_{\text{aux}}(\boldsymbol{v}_h) = (\boldsymbol{g}, \boldsymbol{v}_h)_0 - \sum_{K\in\mathcal{T}_h} \frac{h^2}{\sigma h^2 + 12\nu}(\boldsymbol{g}, \sigma \boldsymbol{v}_h - \nu\Delta \boldsymbol{v}_h)_{0,K}. \tag{27}$$

The unique solvability of the stabilized FEM (25) is ensured by the strong coercivity of the bilinear form $B_{\text{aux}}(\cdot,\cdot)$,

$$B_{\text{aux}}(\boldsymbol{v}_h, \boldsymbol{v}_h) = \nu\|\nabla \boldsymbol{v}_h\|_0^2 + \frac{12\nu\sigma}{\sigma h^2 + 12\nu}\|\boldsymbol{v}_h\|_0^2 \quad \forall\, \boldsymbol{v}_h \in \mathcal{V}_h. \tag{28}$$

Moreover, the convergence of the stabilized finite element solution $\boldsymbol{w}_h$ of (25) can be proved using the similar techniques developed by Franca and Farhat in [22] for a scalar reaction-diffusion problem; see also [40]. We thus state without proof the following lemma:

Lemma 2. *Let $\boldsymbol{w} \in (H_0^1(\Omega) \cap H^2(\Omega))^2$ be the solution of the auxiliary boundary value problem (24). Then the unique stabilized C^0 piecewise linear (or bilinear) finite element solution $\boldsymbol{w}_h$ of (25) converges to $\boldsymbol{w}$ in the following way:*

$$\|\nabla(\boldsymbol{w} - \boldsymbol{w}_h)\|_0^2 + \frac{12\sigma}{\sigma h^2 + 12\nu}\|\boldsymbol{w} - \boldsymbol{w}_h\|_0^2 \le Ch^2\|\boldsymbol{w}\|_2^2. \tag{29}$$

In what follows, we shall present and analyze two finite element solution-projections, respectively associated with velocity $\boldsymbol{u}$ and pressure p. These finite element solution-projections will be used as the intermediate finite element interpolations in the derivation of the error bounds of our stabilization method (5). First, let $\boldsymbol{u} \in (H_0^1(\Omega) \cap H^2(\Omega))^2$ be the exact solution of problem (1). Then we define a source function $\boldsymbol{g}$ by

$$\boldsymbol{g} := \sigma\boldsymbol{u} - \nu\Delta\boldsymbol{u}. \tag{30}$$

Note that $\boldsymbol{u}$ obviously solves the auxiliary boundary value problem (24) with this given source function $\boldsymbol{g}$. As a consequence of Lemma 2, we have following results:

Lemma 3. *Let $\boldsymbol{u} \in (H_0^1(\Omega)\cap H^2(\Omega))^2$ be the solution of problem (1) and $\boldsymbol{w}_h \in \mathcal{V}_h$ the unique solution of (25) associated with the source function $\boldsymbol{g}$ given in (30). Then there exists a constant $C > 0$ independent of ν, σ and h such that*

$$\|\boldsymbol{u} - \boldsymbol{w}_h\|_1 \le Ch\|\boldsymbol{u}\|_2, \tag{31}$$

$$\|\boldsymbol{u} - \boldsymbol{w}_h\|_0 \le Ch\sqrt{\frac{h^2}{12} + \frac{\nu}{\sigma}}\,\|\boldsymbol{u}\|_2. \tag{32}$$

Proof. Since $\boldsymbol{u} \in (H_0^1(\Omega) \cap H^2(\Omega))^2$ and $\boldsymbol{g} := \sigma\boldsymbol{u} - \nu\Delta\boldsymbol{u}$, the exact solution $\boldsymbol{w}$ of the auxiliary boundary value problem (24) is then given by $\boldsymbol{w} = \boldsymbol{u}$. From Lemma 2, we have

$$\|\nabla(\boldsymbol{u} - \boldsymbol{w}_h)\|_0^2 + \frac{12\sigma}{\sigma h^2 + 12\nu}\|\boldsymbol{u} - \boldsymbol{w}_h\|_0^2 \le Ch^2\|\boldsymbol{u}\|_2^2. \tag{33}$$

Combining (33) with the following Poincaré-Friedrichs inequality [7, 9],

$$\|\boldsymbol{v}\|_0 \le C_{pf}\|\nabla\boldsymbol{v}\|_0 \quad \forall\, \boldsymbol{v} \in (H_0^1(\Omega))^2,$$

we can easily obtain the estimate (31). The estimate (32) is a direct consequence of (33). □

We remark that in Lemma 3, since $\boldsymbol{w}_h$ is the stabilized finite element solution of problem (25) with the source function $\boldsymbol{g} := \sigma\boldsymbol{u} - \nu\Delta\boldsymbol{u}$, we have for all $\boldsymbol{v}_h \in \mathcal{V}_h$ that

$$\begin{aligned}
&\sigma(\boldsymbol{w}_h, \boldsymbol{v}_h)_0 + \nu(\nabla\boldsymbol{w}_h, \nabla\boldsymbol{v}_h)_0 - \sum_{K\in\mathcal{T}_h} \frac{h^2}{\sigma h^2 + 12\nu}(\sigma\boldsymbol{w}_h - \nu\Delta\boldsymbol{w}_h, \sigma\boldsymbol{v}_h - \nu\Delta\boldsymbol{v}_h)_{0,K} \\
&= (\boldsymbol{g}, \boldsymbol{v}_h)_0 - \sum_{K\in\mathcal{T}_h} \frac{h^2}{\sigma h^2 + 12\nu}(\boldsymbol{g}, \sigma\boldsymbol{v}_h - \nu\Delta\boldsymbol{v}_h)_{0,K} \\
&= (\sigma\boldsymbol{u} - \nu\Delta\boldsymbol{u}, \boldsymbol{v}_h)_0 - \sum_{K\in\mathcal{T}_h} \frac{h^2}{\sigma h^2 + 12\nu}(\sigma\boldsymbol{u} - \nu\Delta\boldsymbol{u}, \sigma\boldsymbol{v}_h - \nu\Delta\boldsymbol{v}_h)_{0,K} \\
&= \sigma(\boldsymbol{u}, \boldsymbol{v}_h)_0 + \nu(\nabla\boldsymbol{u}, \nabla\boldsymbol{v}_h)_0 - \sum_{K\in\mathcal{T}_h} \frac{h^2}{\sigma h^2 + 12\nu}(\sigma\boldsymbol{u} - \nu\Delta\boldsymbol{u}, \sigma\boldsymbol{v}_h - \nu\Delta\boldsymbol{v}_h)_{0,K}. \qquad (34)
\end{aligned}$$

To give error estimates of the the newly proposed stabilized FEM (5), we also need the following result about the pressure p. A more general form of the result can be found in [9] (see Theorem A.2 on pp. 101-102).

Lemma 4. *Assume that $p \in H^1(\Omega) \cap L_0^2(\Omega)$. Let $\widetilde{p}_h \in Q_h$ be the H^1-seminorm projection of p on the finite element space Q_h, that is,*

$$(\nabla\widetilde{p}_h, \nabla q_h)_0 = (\nabla p, \nabla q_h)_0 \quad \forall\ q_h \in Q_h. \qquad (35)$$

Then there exists a constant $C > 0$ independent of h such that

$$\|p - \widetilde{p}_h\|_0 \le Ch\|p\|_1. \qquad (36)$$

Moreover, if $p \in H^2(\Omega) \cap L_0^2(\Omega)$ then we have

$$h\|\nabla(p - \widetilde{p}_h)\|_0 + \|p - \widetilde{p}_h\|_0 \le Ch^2\|p\|_2. \qquad (37)$$

Now, we are in the position to derive the error estimates of the newly proposed stabilized FEM (5).

Theorem 5. *Let $(\boldsymbol{u}, p) \in (H_0^1(\Omega)\cap H^2(\Omega))^2 \times (H^1(\Omega)\cap L_0^2(\Omega))$ be the solution of problem (1) and $(\boldsymbol{u}_h, p_h) \in \mathcal{V}_h \times Q_h \subseteq (H_0^1(\Omega))^2 \times (H^1(\Omega) \cap L_0^2(\Omega))$ the corresponding stabilized C^0 piecewise linear (or bilinear) finite element solution given by (5). Then there exists a constant $C > 0$ independent of ν, σ and h such that*

$$\begin{aligned}
\|\boldsymbol{u} - \boldsymbol{u}_h\|_0 &\le C\left(\left(h\sqrt{h^2 + \frac{\nu}{\sigma}} + \sqrt{\frac{\nu}{\sigma}}\sqrt{h^2 + \frac{\nu}{\sigma}} + h\sqrt{\frac{\nu}{\sigma}} + \frac{h}{\sqrt{\sigma}}\right)\|\boldsymbol{u}\|_2 + \frac{h}{\sqrt{\sigma}}\|p\|_1\right), \qquad (38)\\
\|\boldsymbol{u} - \boldsymbol{u}_h\|_1 &\le C\left(\left(h + \sqrt{\frac{\nu}{\sigma}} + \frac{\sqrt{\nu}h}{\sqrt{\sigma h^2 + 12\nu}} + \frac{h}{\sqrt{\sigma h^2 + 12\nu}}\right)\|\boldsymbol{u}\|_2 + \frac{h}{\sqrt{\sigma h^2 + 12\nu}}\|p\|_1\right), \qquad (39)\\
\|p - p_h\|_0 &\le C\left(\left(\nu\sqrt{1 + \frac{\nu}{\sigma h^2}} + \nu + \sqrt{\nu}\right)\|\boldsymbol{u}\|_2 + (h + \sqrt{\nu})\|p\|_1\right), \qquad (40)\\
\|\nabla(p - p_h)\|_0 &\le C\left(\|\nabla(p - \widetilde{p}_h)\|_0 + \left(\nu\sqrt{1 + \frac{\nu}{\sigma h^2}} + \nu + \sqrt{\nu}\right)\|\boldsymbol{u}\|_2 + \sqrt{\nu}\|p\|_1\right), \qquad (41)
\end{aligned}$$

where $\widetilde{p}_h \in Q_h$ is the H^1-seminorm projection of p on Q_h given by (35). Moreover, if $p \in H^2(\Omega) \cap L_0^2(\Omega)$ then we have

$$\|p - p_h\|_0 \leq C\left(\left(\nu\sqrt{1+\frac{\nu}{\sigma h^2}} + \nu + \sqrt{\nu}\right)\|\boldsymbol{u}\|_2 + (h^2 + \sqrt{\nu})\|p\|_2\right), \tag{42}$$

$$\|\nabla(p - p_h)\|_0 \leq C\left(\left(\nu\sqrt{1+\frac{\nu}{\sigma h^2}} + \nu + \sqrt{\nu}\right)\|\boldsymbol{u}\|_2 + (h + \sqrt{\nu})\|p\|_2\right). \tag{43}$$

Proof. Let $\boldsymbol{w}_h \in \mathcal{V}_h$ and $\widetilde{p}_h \in Q_h$ be the functions stated in Lemma 3 and Lemma 4, respectively. Utilizing the inf-sup estimate (9) and the orthogonality property (11), we have

$$\begin{aligned}\|(\boldsymbol{u}_h - \boldsymbol{w}_h, p_h - \widetilde{p}_h)\|_h &\leq \sup_{\mathbf{0}\neq(\boldsymbol{v}_h,q_h)\in\mathcal{V}_h\times Q_h} \frac{B((\boldsymbol{u}_h - \boldsymbol{w}_h, p_h - \widetilde{p}_h),(\boldsymbol{v}_h,q_h))}{\|(\boldsymbol{v}_h,q_h)\|_h} \\ &= \sup_{\mathbf{0}\neq(\boldsymbol{v}_h,q_h)\in\mathcal{V}_h\times Q_h} \frac{B((\boldsymbol{u} - \boldsymbol{w}_h, p - \widetilde{p}_h),(\boldsymbol{v}_h,q_h))}{\|(\boldsymbol{v}_h,q_h)\|_h}.\end{aligned} \tag{44}$$

Since $\Delta\boldsymbol{w}_h|_K = 0$ for all $K \in \mathcal{T}_h$ and $\Delta\boldsymbol{v}_h|_K = 0$ for all $\boldsymbol{v}_h \in \mathcal{V}_h$ and $K \in \mathcal{T}_h$, we obtain from Green's formula [9], (34) and (35) that

$$\begin{aligned}
&B((\boldsymbol{u} - \boldsymbol{w}_h, p - \widetilde{p}_h),(\boldsymbol{v}_h,q_h)) \\
&= \sigma(\boldsymbol{u} - \boldsymbol{w}_h, \boldsymbol{v}_h)_0 + \nu(\nabla(\boldsymbol{u} - \boldsymbol{w}_h), \nabla\boldsymbol{v}_h)_0 - (p - \widetilde{p}_h, \nabla\cdot\mathbf{v}_h)_0 - (\nabla\cdot(\boldsymbol{u} - \boldsymbol{w}_h), q_h)_0 \\
&\quad - \sum_{K\in\mathcal{T}_h}\frac{h^2}{\sigma h^2 + 12\nu}(\sigma(\boldsymbol{u} - \boldsymbol{w}_h) - \nu\Delta\boldsymbol{u} + \nabla(p - \widetilde{p}_h), \sigma\boldsymbol{v}_h + \nabla q_h)_{0,K} \\
&\quad + \sum_{K\in\mathcal{T}_h}\frac{12\nu}{\sigma h^2 + 12\nu}(\nabla\cdot(\boldsymbol{u} - \boldsymbol{w}_h), \nabla\cdot\boldsymbol{v}_h)_{0,K} \\
&= \sigma(\boldsymbol{u} - \boldsymbol{w}_h, \boldsymbol{v}_h)_0 + \nu(\nabla(\boldsymbol{u} - \boldsymbol{w}_h), \nabla\boldsymbol{v}_h)_0 + (\nabla(p - \widetilde{p}_h), \boldsymbol{v}_h)_0 + (\boldsymbol{u} - \boldsymbol{w}_h, \nabla q_h)_0 \\
&\quad - \sum_{K\in\mathcal{T}_h}\frac{h^2}{\sigma h^2 + 12\nu}(\sigma(\boldsymbol{u} - \boldsymbol{w}_h) - \nu\Delta\boldsymbol{u} + \nabla(p - \widetilde{p}_h), \sigma\boldsymbol{v}_h + \nabla q_h)_{0,K} \\
&\quad + \sum_{K\in\mathcal{T}_h}\frac{12\nu}{\sigma h^2 + 12\nu}(\nabla\cdot(\boldsymbol{u} - \boldsymbol{w}_h), \nabla\cdot\boldsymbol{v}_h)_{0,K} \\
&= \frac{12\nu}{\sigma h^2 + 12\nu}(\nabla(p - \widetilde{p}_h), \boldsymbol{v}_h)_0 + \frac{12\nu}{\sigma h^2 + 12\nu}(\boldsymbol{u} - \boldsymbol{w}_h, \nabla q_h)_0 - \frac{h^2}{\sigma h^2 + 12\nu}(-\nu\Delta\boldsymbol{u}, \nabla q_h)_0 \\
&\quad + \frac{12\nu}{\sigma h^2 + 12\nu}(\nabla\cdot(\boldsymbol{u} - \boldsymbol{w}_h), \nabla\cdot\boldsymbol{v}_h)_0 \\
&= \frac{12\nu}{\sigma h^2 + 12\nu}(\widetilde{p}_h - p, \nabla\cdot\boldsymbol{v}_h)_0 + \frac{12\nu}{\sigma h^2 + 12\nu}(\boldsymbol{u} - \boldsymbol{w}_h, \nabla q_h)_0 - \frac{h^2}{\sigma h^2 + 12\nu}(-\nu\Delta\boldsymbol{u}, \nabla q_h)_0 \\
&\quad + \frac{12\nu}{\sigma h^2 + 12\nu}(\nabla\cdot(\boldsymbol{u} - \boldsymbol{w}_h), \nabla\cdot\boldsymbol{v}_h)_0.
\end{aligned}$$

Applying Hölder inequality on $B((\boldsymbol{u} - \boldsymbol{w}_h, p - \widetilde{p}_h),(\boldsymbol{v}_h,q_h))$ with (31), (32) and (36), we have

$$\begin{aligned}
B((\boldsymbol{u} - \boldsymbol{w}_h, p - \widetilde{p}_h),(\boldsymbol{v}_h,q_h)) &\leq C\Bigg(\sqrt{\frac{12\nu}{\sigma h^2 + 12\nu}}\|p - \widetilde{p}_h\|_0 + \frac{12\nu}{h\sqrt{\sigma h^2 + 12\nu}}\|\boldsymbol{u} - \boldsymbol{w}_h\|_0 \\
&\quad + \frac{\nu h}{\sqrt{\sigma h^2 + 12\nu}}\|\Delta\boldsymbol{u}\|_0 + \sqrt{\frac{12\nu}{\sigma h^2 + 12\nu}}\|\nabla\cdot(\boldsymbol{u} - \boldsymbol{w}_h)\|_0\Bigg)\|(\boldsymbol{v}_h,q_h)\|_h \\
&\leq C\left(\left(\frac{\nu}{\sqrt{\sigma}} + \frac{\nu h}{\sqrt{\sigma h^2 + 12\nu}} + \frac{\sqrt{\nu}h}{\sqrt{\sigma h^2 + 12\nu}}\right)\|\boldsymbol{u}\|_2 + \frac{\sqrt{\nu}h}{\sqrt{\sigma h^2 + 12\nu}}\|p\|_1\right)\|(\boldsymbol{v}_h,q_h)\|_h.
\end{aligned}$$

Therefore, form (44) and the above estimate, we get

$$|||(\boldsymbol{u}_h - \boldsymbol{w}_h, p_h - \widetilde{p}_h)|||_h \le C\left(\Big(\frac{\nu}{\sqrt{\sigma}} + \frac{\nu h}{\sqrt{\sigma h^2 + 12\nu}} + \frac{\sqrt{\nu} h}{\sqrt{\sigma h^2 + 12\nu}}\Big)\|\boldsymbol{u}\|_2 + \frac{\sqrt{\nu} h}{\sqrt{\sigma h^2 + 12\nu}}\|p\|_1\right),$$

which combined with the definition of energy norm (8) implies

$$\begin{aligned}
\|\nabla(\boldsymbol{u}_h - \boldsymbol{w}_h)\|_0 &\le C\left(\Big(\sqrt{\frac{\nu}{\sigma}} + \frac{\sqrt{\nu} h}{\sqrt{\sigma h^2 + 12\nu}} + \frac{h}{\sqrt{\sigma h^2 + 12\nu}}\Big)\|\boldsymbol{u}\|_2 + \frac{h}{\sqrt{\sigma h^2 + 12\nu}}\|p\|_1\right), && (45)\\
|||(\boldsymbol{u}_h - \boldsymbol{w}_h)|||_0 &\le C\left(\Big(\sqrt{\frac{\nu}{\sigma}}\sqrt{h^2 + \frac{\nu}{\sigma}} + h\sqrt{\frac{\nu}{\sigma}} + \frac{h}{\sqrt{\sigma}}\Big)\|\boldsymbol{u}\|_2 + \frac{h}{\sqrt{\sigma}}\|p\|_1\right), && (46)\\
\|\nabla(p_h - \widetilde{p}_h)\|_0 &\le C\left(\Big(\nu\sqrt{1 + \frac{\nu}{\sigma h^2}} + \nu + \sqrt{\nu}\Big)\|\boldsymbol{u}\|_2 + \sqrt{\nu}\|p\|_1\right). && (47)
\end{aligned}$$

Now the Poincaré-Friedrichs inequality [7, 9] ensures that

$$\begin{aligned}
\|\boldsymbol{u}_h - \boldsymbol{w}_h\|_1 &\le C\left(\Big(\sqrt{\frac{\nu}{\sigma}} + \frac{\sqrt{\nu} h}{\sqrt{\sigma h^2 + 12\nu}} + \frac{h}{\sqrt{\sigma h^2 + 12\nu}}\Big)\|\boldsymbol{u}\|_2 + \frac{h}{\sqrt{\sigma h^2 + 12\nu}}\|p\|_1\right), && (48)\\
\|p_h - \widetilde{p}_h\|_0 &\le C\left(\Big(\nu\sqrt{1 + \frac{\nu}{\sigma h^2}} + \nu + \sqrt{\nu}\Big)\|\boldsymbol{u}\|_2 + \sqrt{\nu}\|p\|_1\right). && (49)
\end{aligned}$$

Finally, combining the triangle inequality with (31), (32), (36), (37) and (45)-(49) yields the conclusion. □

Note that if the family $\{\mathcal{T}_h\}$ of triangulations is quasi-uniform [4, 38, 39], then the error estimates (38)-(40) can be further improved as follows:

Theorem 6. *Let $(\boldsymbol{u}, p) \in (H_0^1(\Omega) \cap H^2(\Omega))^2 \times (H^1(\Omega) \cap L_0^2(\Omega))$ be the solution of problem (1) and $(\boldsymbol{u}_h, p_h) \in \mathcal{V}_h \times \mathcal{Q}_h \subseteq (H_0^1(\Omega))^2 \times (H^1(\Omega) \cap L_0^2(\Omega))$ the corresponding stabilized C^0 piecewise linear (or bilinear) finite element solution given by (5). Assume that the family $\{\mathcal{T}_h\}$ of triangulations is quasi-uniform. Then there exists a constant $C > 0$ independent of ν, σ and h such that*

$$\begin{aligned}
\|\boldsymbol{u} - \boldsymbol{u}_h\|_0 &\le Ch\left(\Big(h + \sqrt{\frac{\nu}{\sigma}} + \frac{1}{\sqrt{\sigma}}\Big)\|\boldsymbol{u}\|_2 + \frac{1}{\sqrt{\sigma}}\|p\|_1\right), && (50)\\
\|\boldsymbol{u} - \boldsymbol{u}_h\|_1 &\le Ch\left(\Big(1 + \frac{1}{\sqrt{\sigma h^2 + 12\nu}}\Big)\|\boldsymbol{u}\|_2 + \frac{1}{\sqrt{\sigma h^2 + 12\nu}}\|p\|_1\right), && (51)\\
\|p - p_h\|_0 &\le C\left((\nu + \sqrt{\nu})\|\boldsymbol{u}\|_2 + (h + \sqrt{\nu})\|p\|_1\right). && (52)
\end{aligned}$$

Proof. The proof is very similar to that of Theorem 5, except we replace the finite element solution-projection $\boldsymbol{w}_h \in \mathcal{V}_h$ stated in Lemma 3 with the usual L^2 projection of $\boldsymbol{u}$ onto $\mathcal{V}_h$. That is, let $\boldsymbol{w}_h$ be the solution of

$$(\boldsymbol{u} - \boldsymbol{w}_h, \boldsymbol{v}_h)_0 = 0 \quad \forall\, \boldsymbol{v}_h \in \mathcal{V}_h.$$

Since the family $\{\mathcal{T}_h\}$ of triangulations is quasi-uniform, we have (cf. [4, 38, 39])

$$\|\boldsymbol{u} - \boldsymbol{w}_h\|_0 \le Ch^2\|\boldsymbol{u}\|_2 \quad \text{and} \quad \|\nabla(\boldsymbol{u} - \boldsymbol{w}_h)\|_0 \le Ch\|\boldsymbol{u}\|_2.$$

With a suitable adjustment in the argument for proving Theorem 5, we obtain

$$|||(\boldsymbol{u}_h - \boldsymbol{w}_h, p_h - \widetilde{p}_h)|||_h \le C\left(\Big(\sqrt{\nu}h + \frac{\nu h}{\sqrt{\sigma h^2 + 12\nu}} + \frac{\sqrt{\nu}h}{\sqrt{\sigma h^2 + 12\nu}}\Big)\|\boldsymbol{u}\|_2 + \frac{\sqrt{\nu}h}{\sqrt{\sigma h^2 + 12\nu}}\|p\|_1\right). \tag{53}$$

Similar to that in Theorem 5, estimates (50) and (51) can be immediately derived from (53). On the other hand, combining the Poincaré-Friedrichs inequality with (8), (53) and (47), we get that

$$\begin{aligned}
\|p_h - \widetilde{p}_h\|_0 &\le C\|\nabla(p_h - \widetilde{p}_h)\|_0 \\
&\le C\left((\nu + \sqrt{\nu})\|\boldsymbol{u}\|_2 + \min\left\{\nu\sqrt{1 + \frac{\nu}{\sigma h^2}}, \nu\sqrt{1 + \frac{\sigma h^2}{\nu}}\right\}\|\boldsymbol{u}\|_2 + \sqrt{\nu}\|p\|_1\right) \\
&\le C\left((\nu + \sqrt{\nu})\|\boldsymbol{u}\|_2 + \sqrt{\nu}\|p\|_1\right).
\end{aligned} \tag{54}$$

Now, estimate (52) follows from (54) with the triangle inequality and (36). □

From the error estimates (38)-(43) and (50)-(52), we can find that the proposed stabilized FEM (5) using C^0 piecewise P_1-P_1 (or Q_1-Q_1) elements is particularly suitable for the generalized Stokes system (1) with a small viscosity ν and a large reaction coefficient σ. To the best of our knowledge, they have never been achieved before in the error analysis of other stabilization methods in the literature.

Remark 3. In practical computations, there usually holds $\nu \le 1 \le \sigma h^2$ for a certain range of h or the time step $\delta t = h^2$ (i.e., $\sigma = \delta t^{-1} = h^{-2}$) for all h. With this assumption, (38) and (39) can be rewritten as

$$\|\boldsymbol{u} - \boldsymbol{u}_h\|_0 \le Ch^2(\|\boldsymbol{u}\|_2 + \|p\|_1), \tag{55}$$

$$\|\boldsymbol{u} - \boldsymbol{u}_h\|_1 \le Ch(\|\boldsymbol{u}\|_2 + \|p\|_1), \tag{56}$$

where $C > 0$ is independent of ν, σ and h. Note that, in (55), it does not require the usual assumption of a convex domain. Also, note that no quasi-uniform meshes are required in (55) and (56).

Remark 4. From the continuous inf-sup condition [7],

$$\sup_{\mathbf{0}\neq\boldsymbol{v}\in(H_0^1(\Omega))^2} \frac{(\nabla\cdot\boldsymbol{v}, q)_0}{\|\boldsymbol{v}\|_1} \ge C\|q\|_0 \quad \forall\, q \in L_0^2(\Omega),$$

and (50), (51) and (54), we can further prove that

$$\begin{aligned}
\|p_h - \widetilde{p}_h\|_0 \le\ & C\Big(h\|\boldsymbol{u}\|_2 + h\|p\|_1 + h(\nu + \sqrt{\nu})\|\boldsymbol{u}\|_2 + h\sqrt{\nu}\|p\|_1 \\
& + h\Big(\frac{1}{\sqrt{\sigma h^2 + 12\nu}} + \sqrt{\sigma h^2 + 12\nu} + \sqrt{\sigma h} + \sigma h + \sqrt{\sigma\nu}\Big)\|\boldsymbol{u}\|_2 \\
& + h\Big(\frac{1}{\sqrt{\sigma h^2 + 12\nu}} + \sqrt{\sigma h^2 + 12\nu} + \sqrt{\sigma h}\Big)\|p\|_1\Big),
\end{aligned}$$

which combined with the triangle inequality and (36) leads to

$$\begin{aligned}\|p-p_h\|_0 \;\leq\; Ch\Big(&\|\boldsymbol{u}\|_2+\|p\|_1+(\nu+\sqrt{\nu})\|\boldsymbol{u}\|_2+\sqrt{\nu}\|p\|_1\\&+\Big(\frac{1}{\sqrt{\sigma h^2+12\nu}}+\sqrt{\sigma h^2+12\nu}+\sqrt{\sigma h}+\sigma h+\sqrt{\sigma\nu}\Big)\|\boldsymbol{u}\|_2\\&+\Big(\frac{1}{\sqrt{\sigma h^2+12\nu}}+\sqrt{\sigma h^2+12\nu}+\sqrt{\sigma h}\Big)\|p\|_1\Big).\end{aligned}\tag{57}$$

Note that, in (57), the reaction coefficient σ is controlled by a factor h or a factor ν. *Also, note that* $\|p-p_h\|_0$ *is bounded by the minimum of the right-hand sides of (52) and (57).*

Remark 5. We remark that if $\sigma h^2 \gg \nu$ and $0<\nu\ll 1$ then it is reasonable to neglect the div-div stabilization term in the stabilized FEM (5) and in such case, method (5) will be reduced to the Barrenechea-Valentin stabilized FEM (16), provided the mesh size h is replaced by the element-dependent parameter h_K. However, without the divergence-free stabilization effect, we are only able to derive less sharp error estimates than those obtained in Theorem 5. For example, with a suitable adjustment in the argument for proving Theorem 5, we can only obtain

$$\|\boldsymbol{u}-\boldsymbol{u}_h\|_1 \leq C\left(h+\frac{1}{\sigma h}+\sqrt{\frac{\nu}{\sigma}}\right)(\|\boldsymbol{u}\|_2+\|p\|_1),\tag{58}$$

where the term $1/\sigma h$ will dominate in some cases. That is why we need to keep the div-div stabilization term in method (5) even if the associated stabilization parameter $12\nu/(\sigma h^2+12\nu)$ is very small when $\sigma h^2\gg\nu$ and $0<\nu\ll 1$. Finally, we like to emphasize that, with the div-div stabilization term in (5), the error estimates given in Theorem 5 are valid for the entire range of the viscosity $0<\nu\leq 1$ as well as the entire range of the reaction coefficient $\sigma\geq 1$. Note that σ is inversely proportional to the time step δt.

Remark 6. Note that the stabilization parameters of the proposed stabilized FEM (5) is only designed for the C^0 piecewise P_1-P_1 (or Q_1-Q_1) elements. If the higher-order finite elements are used, the stabilization parameters in the method need to be redesigned. Indeed, quite similar to (19), we may design the two stabilization parameters as

$$\frac{h^2}{\sigma h^2+(4\nu/C_k)}\quad\text{and}\quad\frac{(4\nu/C_k)}{\sigma h^2+(4\nu/C_k)},\tag{59}$$

where constant C_k takes value according to the local inverse inequality,

$$C_k h_K^2\|\Delta v_h\|_{0,K}^2\leq\|\nabla v_h\|_{0,K}^2\quad\forall\, v_h\in V_k, k\geq 2,$$

and $V_k\subseteq H_0^1(\Omega)$ denotes the C^0 piecewise P_k finite element space. For example of $k=2$, from [15] for various orders of finite elements, one can find that $C_2=1/48$. Thus, if $\sigma h^2\gg\nu$ and $0<\nu\ll 1$ then our stabilization parameters in method (5) should be replaced by

$$\frac{h^2}{\sigma h^2+192\nu}\quad\text{and}\quad\frac{192\nu}{\sigma h^2+192\nu}.$$

In the Example 1 of Section 4 below, we will provide some numerical results of the proposed stabilized FEM (5) with the above new stabilization parameters and using C^0 piecewise P_2-P_2 elements to verify its validness.

Remark 7. The stabilization parameters in our stabilized FEM (5) are fixed and element-independent. This somehow prevents the use of adaptive meshes. Based on our recent numerical experiences, for an adaptive mesh, it should be better to use element-dependent stabilization parameters, i.e., replacing h by h_K in the parameters. However, as is often seen in the literature of stabilized FEMs, adaptive mesh computation seems to be generally unnecessary for an effective stabilized FEM because accurate results can be already obtained even for boundary or interior layer problems; see also an example depicted in Figure 11 below.

4. Numerical experiments

This section is devoted to numerical experiments to illustrate the super performance of the proposed stabilized FEM (5) for the generalized Stokes system (1) with a small viscosity and a large reaction coefficient. The performance of the proposed stabilized FEM (5) will be also evaluated against the results from the Barrenechea-Blasco (BB) method (12), the Barrenechea-Valentin (BV) method (16), and the Bochev-Gunzburger-Lehoucq (BGL) method (20). We will consider four test problems that are used in [1, 17, 30]. The relative errors of numerical solutions of the first example will be calculated and the convergence rates will be estimated. By comparing the accuracy and stability, we may conclude that the present stabilized FEM (5) achieves better results than the Barrenechea-Blasco method and the Bochev-Gunzburger-Lehoucq method while comparable with the Barrenechea-Valentin method when $\sigma h^2 \gg \nu$ and $0 < \nu \ll 1$.

Example 1. (P_1-P_1 *and* P_2-P_2 *finite elements*) This example is quoted from [17]. We will first study the detailed convergence behavior of various stabilized FEMs with P_1-P_1 finite elements on the unit square domain $\Omega = (0,1) \times (0,1)$. We assume that the smooth exact solution $(\boldsymbol{u}, p)$ of problem (1) is given by

$$\begin{aligned} u_1(x,y) &= -256x^2(x-1)^2y(y-1)(2y-1), \\ u_2(x,y) &= -u_1(y,x), \\ p(x,y) &= 150(x-1/2)(y-1/2). \end{aligned}$$

Substituting the solution $(\boldsymbol{u}, p)$ into problem (1), we obtain the source-like function $\boldsymbol{f}$. Notice that $\boldsymbol{u} = \boldsymbol{0}$ on $\partial\Omega$ and $\int_\Omega p = 0$. We concentrate on the uniform triangular meshes of Ω. Here, a uniform triangular mesh is formed by dividing each square, with side-length h^* in a uniform square mesh, into two triangles by drawing a diagonal line from the left-down corner to the right-up corner. Thus, we have $h_K = h = \sqrt{2}h^*$ for all $K \in \mathcal{T}_h$.

Numerical results for $\nu = 10^{-\ell}$, $\ell = 2, 3, 4$, and $\sigma = 10^m$, $m = 2, 3, 4, 5$, are reported in Table 1 - Table 8, where the convergence orders are estimated. From the numerical results, we may observe the following:

- The newly proposed stabilized FEM (5) using P_1-P_1 finite elements displays optimal orders of convergence in the L^2 norm and H^1 norm for both velocity field and pressure. Moreover, the convergence behavior are independent of the small viscosity ν and the large reaction coefficient σ. These observations are consistent with the theoretical analysis given in Theorem 5 and Theorem 6. More importantly, the proposed method (5) also

presents a robust behavior in the sense that no pressure instabilities appear, even if we use a rather coarse mesh with $h^* = 1/20$; see Figure 1 for the contours of pressure approximations.

- The Barrenechea-Valentin method (16) can produce robust results. Their convergence behavior are very similar to those of the newly proposed stabilized FEM (5) when $\sigma h^2 \gg \nu$ and $0 < \nu \ll 1$.

- On the contrast, the convergence behavior of the Barrenechea-Blasco method (12) and the Bochev-Gunzburger-Lehoucq method (20) are obviously dependent on the reaction coefficient σ. The accuracy and stability of both methods are deteriorated when the reaction coefficient σ is getting larger. Meanwhile, the pressure oscillations appear; see Figure 1.

The results depicted in Figure 1 are using a uniform triangulation with $h^* = 1/20$. For further testing the performance of various stabilized FEMs, we next consider the P_1-P_1 finite elements on an unstructured triangular mesh that is depicted in Figure 2. This mesh is constructed by dividing each side of the square Ω into equal segments with length $h^* = 1/20$ and then using the *FreeFem++* (see [42]) to generate an unstructured quasi-uniform mesh. In the numerical simulation of the present stabilized FEM, the mesh parameter h is taken as $h = h^* = 1/20$. The contour plots of pressure approximations produced by various stabilized FEMs are displayed in Figure 3. Again, one can find that the present stabilized FEM (5) and the Barrenechea-Valentin method (16) generate more accurate results with a better stability than the numerical results produced by the other two stabilized FEMs when $0 < \nu \ll 1$ and $\sigma \gg 1$.

We now consider the proposed stabilized FEM (5) with the new stabilization parameters described in Remark 6 and using C^0 piecewise P_2-P_2 finite elements on the uniform triangular meshes. The numerical results are reported in Table 9 and Table 10. In this case, our stabilization method still shows superior accuracy and stability. We remark that the Barrenechea-Valentin stabilized method using P_2-P_2 finite elements exhibits the similar behavior.

Table 1. L^2 relative errors of $\boldsymbol{u}_h$ and p_h produced by the proposed stabilized FEM (5) using P_1-P_1 finite elements for Example 1 with various viscosity ν and reaction coefficient σ.

L^2 error	ν	σ	h^* = 1/20	1/40	1/60	1/80	1/100	order
$\boldsymbol{u}_h$	10^{-2}	10^2	2.8661e-2	7.3342e-3	3.2841e-3	1.8549e-3	1.1904e-3	1.98
		10^3	2.6070e-2	6.6626e-3	2.9812e-3	1.6828e-3	1.0794e-3	1.98
		10^4	2.5901e-2	6.6352e-3	2.9711e-3	1.6772e-3	1.0757e-3	1.98
		10^5	2.5889e-2	6.6367e-3	2.9734e-3	1.6791e-3	1.0771e-3	1.98
$\boldsymbol{u}_h$	10^{-3}	10^2	2.8738e-2	7.3559e-3	3.2918e-3	1.8578e-3	1.1916e-3	1.98
		10^3	2.6073e-2	6.6626e-3	2.9803e-3	1.6816e-3	1.0782e-3	1.98
		10^4	2.5902e-2	6.6353e-3	2.9711e-3	1.6772e-3	1.0756e-3	1.98
		10^5	2.5889e-2	6.6367e-3	2.9734e-3	1.6791e-3	1.0771e-3	1.98
$\boldsymbol{u}_h$	10^{-4}	10^2	2.8746e-2	7.3587e-3	3.2931e-3	1.8584e-3	1.1916e-3	1.98
		10^3	2.6074e-2	6.6626e-3	2.9802e-3	1.6815e-3	1.0780e-3	1.98
		10^4	2.5902e-2	6.6353e-3	2.9711e-3	1.6772e-3	1.0756e-3	1.98
		10^5	2.5889e-2	6.6367e-3	2.9734e-3	1.6791e-3	1.0771e-3	1.98
p_h	10^{-2}	10^2	4.1816e-3	8.3636e-4	3.3515e-4	1.9508e-4	1.3661e-4	2.01
		10^3	4.6320e-3	1.1110e-3	4.6547e-4	2.4804e-4	1.5393e-4	2.13
		10^4	4.6973e-3	1.1755e-3	5.2090e-4	2.9182e-4	1.8604e-4	2.01
		10^5	4.7042e-3	1.1829e-3	5.2810e-4	2.9870e-4	1.9248e-4	1.98
p_h	10^{-3}	10^2	4.6380e-3	1.1155e-3	4.6547e-4	2.4273e-4	1.4367e-4	2.21
		10^3	4.6931e-3	1.1710e-3	5.1619e-4	2.8689e-4	1.8085e-4	2.03
		10^4	4.6998e-3	1.1784e-3	5.2365e-4	2.9426e-4	1.8805e-4	2.00
		10^5	4.7005e-3	1.1792e-3	5.2444e-4	2.9506e-4	1.8884e-4	2.00
p_h	10^{-4}	10^2	4.6942e-3	1.1723e-3	5.1751e-4	2.8816e-4	1.8204e-4	2.03
		10^3	4.6998e-3	1.1784e-3	5.2362e-4	2.9423e-4	1.8802e-4	2.00
		10^4	4.7005e-3	1.1791e-3	5.2439e-4	2.9501e-4	1.8880e-4	2.00
		10^5	4.7005e-3	1.1792e-3	5.2447e-4	2.9509e-4	1.8888e-4	2.00

Table 2. H^1 relative errors of $\boldsymbol{u}_h$ and p_h produced by the proposed stabilized FEM (5) using P_1-P_1 finite elements for Example 1 with various viscosity ν and reaction coefficient σ.

H^1 error	ν	σ	$h^* = 1/20$	$1/40$	$1/60$	$1/80$	$1/100$	order
$\boldsymbol{u}_h$	10^{-2}	10^2	1.3861e-1	6.9221e-2	4.6113e-2	3.4571e-2	2.7650e-2	1.00
		10^3	1.3872e-1	6.9284e-2	4.6150e-2	3.4595e-2	2.7666e-2	1.00
		10^4	1.3884e-1	6.9334e-2	4.6176e-2	3.4611e-2	2.7678e-2	1.00
		10^5	1.3886e-1	6.9349e-2	4.6186e-2	3.4619e-2	2.7684e-2	1.00
$\boldsymbol{u}_h$	10^{-3}	10^2	1.3866e-1	6.9257e-2	4.6138e-2	3.4588e-2	2.7663e-2	1.00
		10^3	1.3872e-1	6.9289e-2	4.6155e-2	3.4599e-2	2.7671e-2	1.00
		10^4	1.3884e-1	6.9334e-2	4.6176e-2	3.4612e-2	2.7679e-2	1.00
		10^5	1.3886e-1	6.9349e-2	4.6187e-2	3.4619e-2	2.7684e-2	1.00
$\boldsymbol{u}_h$	10^{-4}	10^2	1.3866e-1	6.9263e-2	4.6143e-2	3.4593e-2	2.7667e-2	1.00
		10^3	1.3872e-1	6.9289e-2	4.6155e-2	3.4600e-2	2.7671e-2	1.00
		10^4	1.3884e-1	6.9334e-2	4.6176e-2	3.4612e-2	2.7679e-2	1.00
		10^5	1.3886e-1	6.9349e-2	4.6187e-2	3.4619e-2	2.7684e-2	1.00
p_h	10^{-2}	10^2	6.9005e-2	3.4616e-2	2.3100e-2	1.7335e-2	1.3875e-2	1.00
		10^3	6.9000e-2	3.4607e-2	2.3091e-2	1.7327e-2	1.3868e-2	1.00
		10^4	6.8999e-2	3.4603e-2	2.3086e-2	1.7320e-2	1.3860e-2	1.00
		10^5	6.8999e-2	3.4603e-2	2.3084e-2	1.7318e-2	1.3857e-2	1.00
p_h	10^{-3}	10^2	6.8994e-2	3.4599e-2	2.3081e-2	1.7315e-2	1.3854e-2	1.00
		10^3	6.8994e-2	3.4599e-2	2.3080e-2	1.7315e-2	1.3853e-2	1.00
		10^4	6.8994e-2	3.4599e-2	2.3080e-2	1.7314e-2	1.3853e-2	1.00
		10^5	6.8994e-2	3.4599e-2	2.3080e-2	1.7314e-2	1.3853e-2	1.00
p_h	10^{-4}	10^2	6.8994e-2	3.4599e-2	2.3080e-2	1.7314e-2	1.3853e-2	1.00
		10^3	6.8994e-2	3.4599e-2	2.3080e-2	1.7314e-2	1.3853e-2	1.00
		10^4	6.8994e-2	3.4599e-2	2.3080e-2	1.7314e-2	1.3853e-2	1.00
		10^5	6.8994e-2	3.4599e-2	2.3080e-2	1.7314e-2	1.3853e-2	1.00

Table 3. L^2 relative errors of $\boldsymbol{u}_h$ and p_h produced by the Barrenechea-Blasco stabilized FEM (12) using P_1-P_1 finite elements for Example 1 with various viscosity ν and reaction coefficient σ, where we take $\alpha = 0.0125\nu$ in (15).

L^2 error	ν	σ	$h^* = 1/20$	1/40	1/60	1/80	1/100	order
$\boldsymbol{u}_h$	10^{-2}	10^2	8.6701e-3	1.9436e-3	8.2304e-4	4.5120e-4	2.8416e-4	2.11
		10^3	7.7031e-3	1.8012e-3	7.7896e-4	4.3105e-4	2.7273e-4	2.07
		10^4	7.4258e-3	1.7339e-3	7.5176e-4	4.1744e-4	2.6502e-4	2.06
		10^5	7.7614e-3	1.7195e-3	7.4236e-4	4.1180e-4	2.6137e-4	2.08
$\boldsymbol{u}_h$	10^{-3}	10^2	8.9676e-3	2.0836e-3	8.8730e-4	4.8297e-4	3.0112e-4	2.11
		10^3	7.7121e-3	1.8082e-3	7.8481e-4	4.3587e-4	2.7665e-4	2.06
		10^4	7.4265e-3	1.7344e-3	7.5215e-4	4.1778e-4	2.6533e-4	2.06
		10^5	7.7595e-3	1.7194e-3	7.4238e-4	4.1182e-4	2.6139e-4	2.08
$\boldsymbol{u}_h$	10^{-4}	10^2	9.0125e-3	2.1243e-3	9.2142e-4	5.1045e-4	3.2281e-4	2.06
		10^3	7.7130e-3	1.8090e-3	7.8562e-4	4.3667e-4	2.7742e-4	2.06
		10^4	7.4265e-3	1.7345e-3	7.5219e-4	4.1782e-4	2.6537e-4	2.06
		10^5	7.7593e-3	1.7194e-3	7.4238e-4	4.1182e-4	2.6139e-4	2.08
p_h	10^{-2}	10^2	9.1507e-3	2.5278e-3	1.2432e-3	7.6091e-4	5.2473e-4	1.74
		10^3	1.4595e-2	3.4338e-3	1.5381e-3	8.9108e-4	5.9263e-4	1.95
		10^4	2.1717e-2	7.3508e-3	2.9011e-3	1.5246e-3	9.4269e-4	2.06
		10^5	1.8790e+0	3.6349e-2	5.2678e-3	4.7110e-3	3.0482e-3	3.20
p_h	10^{-3}	10^2	8.3593e-3	2.0200e-3	9.2813e-4	5.4874e-4	3.6966e-4	1.89
		10^3	1.4519e-2	3.3460e-3	1.4535e-3	8.1192e-4	5.1963e-4	2.05
		10^4	2.2280e-2	7.4249e-3	2.9074e-3	1.5139e-3	9.2639e-4	2.09
		10^5	1.8750e+0	3.4888e-2	5.8043e-3	5.0084e-3	3.2260e-3	3.16
p_h	10^{-4}	10^2	8.2566e-3	1.9187e-3	8.3728e-4	4.7009e-4	3.0272e-4	2.03
		10^3	1.4512e-2	3.3368e-3	1.4440e-3	8.0237e-4	5.1012e-4	2.06
		10^4	2.2338e-2	7.4325e-3	2.9081e-3	1.5128e-3	9.2470e-4	2.09
		10^5	1.8746e+0	3.4746e-2	5.8645e-3	5.0405e-3	3.2453e-3	3.16

Table 4. H^1 relative errors of $\boldsymbol{u}_h$ and p_h produced by the Barrenechea-Blasco stabilized FEM (12) using P_1-P_1 finite elements for Example 1 with various viscosity ν and reaction coefficient σ, where we take $\alpha = 0.0125\nu$ in (15).

H^1 error	ν	σ	$h^* = 1/20$	$1/40$	$1/60$	$1/80$	$1/100$	order
$\boldsymbol{u}_h$	10^{-2}	10^2	1.4534e-1	7.1145e-2	4.7005e-2	3.5090e-2	2.7991e-2	1.02
		10^3	1.4236e-1	7.0451e-2	4.6783e-2	3.5001e-2	2.7950e-2	1.01
		10^4	1.4111e-1	6.9950e-2	4.6497e-2	3.4821e-2	2.7831e-2	1.01
		10^5	1.4019e-1	6.9708e-2	4.6358e-2	3.4723e-2	2.7757e-2	1.01
$\boldsymbol{u}_h$	10^{-3}	10^2	1.4728e-1	7.2780e-2	4.8127e-2	3.5853e-2	2.8528e-2	1.02
		10^3	1.4245e-1	7.0552e-2	4.6896e-2	3.5119e-2	2.8066e-2	1.01
		10^4	1.4113e-1	6.9959e-2	4.6506e-2	3.4831e-2	2.7842e-2	1.01
		10^5	1.4019e-1	6.9710e-2	4.6359e-2	3.4724e-2	2.7758e-2	1.01
$\boldsymbol{u}_h$	10^{-4}	10^2	1.4756e-1	7.3231e-2	4.8665e-2	3.6414e-2	2.9071e-2	1.01
		10^3	1.4246e-1	7.0564e-2	4.6911e-2	3.5136e-2	2.8087e-2	1.01
		10^4	1.4113e-1	6.9960e-2	4.6507e-2	3.4832e-2	2.7843e-2	1.01
		10^5	1.4019e-1	6.9710e-2	4.6359e-2	3.4724e-2	2.7758e-2	1.01
p_h	10^{-2}	10^2	1.4161e-1	7.6863e-2	5.5806e-2	4.5025e-2	3.8473e-2	0.78
		10^3	1.9289e-1	9.7568e-2	6.6418e-2	5.1413e-2	4.2693e-2	0.91
		10^4	1.4308e-1	1.3227e-1	9.5099e-2	7.3367e-2	5.9728e-2	0.69
		10^5	4.3665e+0	1.7521e-1	5.8779e-2	8.1402e-2	7.8860e-2	1.59
p_h	10^{-3}	10^2	1.3210e-1	6.4421e-2	4.4056e-2	3.4345e-2	2.8616e-2	0.91
		10^3	1.9239e-1	9.5588e-2	6.3313e-2	4.7427e-2	3.8029e-2	1.00
		10^4	1.4434e-1	1.3227e-1	9.4602e-2	7.2506e-2	5.8554e-2	0.71
		10^5	4.3565e+0	1.7227e-1	5.9684e-2	8.1834e-2	7.9040e-2	1.58
p_h	10^{-4}	10^2	1.3087e-1	6.2004e-2	4.0794e-2	3.0556e-2	2.4556e-2	1.02
		10^3	1.9234e-1	9.5378e-2	6.2963e-2	4.6946e-2	3.7423e-2	1.02
		10^4	1.4447e-1	1.3227e-1	9.4551e-2	7.2417e-2	5.8431e-2	0.71
		10^5	4.3555e+0	1.7198e-1	5.9780e-2	8.1878e-2	7.9058e-2	1.58

Table 5. L^2 relative errors of $\boldsymbol{u}_h$ and p_h produced by the Barrenechea-Valentin stabilized FEM (16) using P_1-P_1 finite elements for Example 1 with various viscosity ν and reaction coefficient σ.

L^2 error	ν	σ	h^* = 1/20	1/40	1/60	1/80	1/100	order
$\boldsymbol{u}_h$	10^{-2}	10^2	2.5919e-2	6.6300e-3	2.0264e-3	1.0281e-3	6.3035e-4	2.36
		10^3	2.5884e-2	6.6360e-3	2.9731e-3	1.6789e-3	1.0770e-3	1.98
		10^4	2.5887e-2	6.6369e-3	2.9737e-3	1.6794e-3	1.0774e-3	1.98
		10^5	2.5888e-2	6.6371e-3	2.9738e-3	1.6795e-3	1.0774e-3	1.98
$\boldsymbol{u}_h$	10^{-3}	10^2	2.5997e-2	6.6707e-3	2.9880e-3	1.6862e-3	1.0807e-3	1.98
		10^3	2.5888e-2	6.6373e-3	2.9739e-3	1.6796e-3	1.0775e-3	1.98
		10^4	2.5888e-2	6.6371e-3	2.9738e-3	1.6795e-3	1.0774e-3	1.98
		10^5	2.5888e-2	6.6371e-3	2.9738e-3	1.6795e-3	1.0774e-3	1.98
$\boldsymbol{u}_h$	10^{-4}	10^2	2.6006e-2	6.6777e-3	2.9945e-3	1.6919e-3	1.0857e-3	1.98
		10^3	2.5889e-2	6.6375e-3	2.9740e-3	1.6796e-3	1.0775e-3	1.98
		10^4	2.5888e-2	6.6371e-3	2.9738e-3	1.6795e-3	1.0774e-3	1.98
		10^5	2.5888e-2	6.6371e-3	2.9738e-3	1.6795e-3	1.0774e-3	1.98
p_h	10^{-2}	10^2	4.0837e-3	7.6276e-4	2.4838e-4	1.2803e-4	7.9730e-5	2.40
		10^3	4.6297e-3	1.1057e-3	4.5659e-4	2.3535e-4	1.3768e-4	2.24
		10^4	4.6972e-3	1.1752e-3	5.2024e-4	2.9080e-4	1.8463e-4	2.02
		10^5	4.7042e-3	1.1828e-3	5.2804e-4	2.9862e-4	1.9236e-4	1.98
p_h	10^{-3}	10^2	4.6254e-3	1.1014e-3	4.5253e-4	2.3156e-4	1.3419e-4	2.26
		10^3	4.6929e-3	1.1708e-3	5.1587e-4	2.8650e-4	1.8040e-4	2.04
		10^4	4.6998e-3	1.1784e-3	5.2364e-4	2.9425e-4	1.8803e-4	2.00
		10^5	4.7005e-3	1.1792e-3	5.2444e-4	2.9506e-4	1.8884e-4	2.00
p_h	10^{-4}	10^2	4.6929e-3	1.1708e-3	5.1583e-4	2.8646e-4	1.8035e-4	2.04
		10^3	4.6998e-3	1.1784e-3	5.2360e-4	2.9421e-4	1.8799e-4	2.00
		10^4	4.7005e-3	1.1791e-3	5.2439e-4	2.9501e-4	1.8880e-4	2.00
		10^5	4.7005e-3	1.1792e-3	5.2447e-4	2.9509e-4	1.8888e-4	2.00

Table 6. H^1 relative errors of $\boldsymbol{u}_h$ and p_h produced by the Barrenechea-Valentin stabilized FEM (16) using P_1-P_1 finite elements for Example 1 with various viscosity ν and reaction coefficient σ.

H^1 error	ν	σ	$h^* = 1/20$	$1/40$	$1/60$	$1/80$	$1/100$	order
$\boldsymbol{u}_h$	10^{-2}	10^2	1.3891e-1	6.9326e-2	4.6071e-2	3.4547e-2	2.7636e-2	1.00
		10^3	1.3886e-1	6.9345e-2	4.6183e-2	3.4615e-2	2.7680e-2	1.00
		10^4	1.3886e-1	6.9350e-2	4.6188e-2	3.4612e-2	2.7685e-2	1.00
		10^5	1.3886e-1	6.9351e-2	4.6189e-2	3.4621e-2	2.7685e-2	1.00
$\boldsymbol{u}_h$	10^{-3}	10^2	1.3900e-1	6.9412e-2	4.6220e-2	3.4637e-2	2.7694e-2	1.00
		10^3	1.3886e-1	6.9351e-2	4.6188e-2	3.4620e-2	2.7685e-2	1.00
		10^4	1.3886e-1	6.9351e-2	4.6189e-2	3.4621e-2	2.7685e-2	1.00
		10^5	1.3886e-1	6.9351e-2	4.6189e-2	3.4621e-2	2.7686e-2	1.00
$\boldsymbol{u}_h$	10^{-4}	10^2	1.3901e-1	6.9428e-2	4.6239e-2	3.4658e-2	2.7714e-2	1.00
		10^3	1.3886e-1	6.9352e-2	4.6189e-2	3.4621e-2	2.7686e-2	1.00
		10^4	1.3886e-1	6.9351e-2	4.6189e-2	3.4621e-2	2.7686e-2	1.00
		10^5	1.3886e-1	6.9351e-2	4.6189e-2	3.4621e-2	2.7686e-2	1.00
p_h	10^{-2}	10^2	6.9001e-2	3.4606e-2	2.3085e-2	1.7317e-2	1.3855e-2	1.00
		10^3	6.8998e-2	3.4602e-2	2.3084e-2	1.7318e-2	1.3856e-2	1.00
		10^4	6.8999e-2	3.4603e-2	2.3084e-2	1.7318e-2	1.3856e-2	1.00
		10^5	6.8999e-2	3.4603e-2	2.3084e-2	1.7318e-2	1.3856e-2	1.00
p_h	10^{-3}	10^2	6.8994e-2	3.4599e-2	2.3081e-2	1.7315e-2	1.3853e-2	1.00
		10^3	6.8994e-2	3.4599e-2	2.3080e-2	1.7314e-2	1.3853e-2	1.00
		10^4	6.8994e-2	3.4599e-2	2.3080e-2	1.7314e-2	1.3853e-2	1.00
		10^5	6.8994e-2	3.4599e-2	2.3080e-2	1.7314e-2	1.3853e-2	1.00
p_h	10^{-4}	10^2	6.8994e-2	3.4599e-2	2.3080e-2	1.7314e-2	1.3853e-2	1.00
		10^3	6.8994e-2	3.4599e-2	2.3080e-2	1.7314e-2	1.3853e-2	1.00
		10^4	6.8994e-2	3.4599e-2	2.3080e-2	1.7314e-2	1.3853e-2	1.00
		10^5	6.8994e-2	3.4599e-2	2.3080e-2	1.7314e-2	1.3853e-2	1.00

Table 7. L^2 relative errors of $\boldsymbol{u}_h$ and p_h produced by the Bochev-Gunzburger-Lehoucq stabilized FEM (20) using P_1-P_1 finite elements for Example 1 with various viscosity ν and reaction coefficient σ, where we take $\delta = 0.05$ in (23).

L^2 error	ν	σ	$h^* = 1/20$	1/40	1/60	1/80	1/100	order
$\boldsymbol{u}_h$	10^{-2}	10^2	7.8793e-3	1.8241e-3	7.8577e-4	4.3469e-4	2.7537e-4	2.07
		10^3	7.4884e-3	1.7497e-3	7.5763e-4	4.2005e-4	2.6631e-4	2.06
		10^4	7.4842e-3	1.7189e-3	7.4412e-4	4.1301e-4	2.6218e-4	2.07
		10^5	8.9021e-3	1.7630e-3	7.4492e-4	4.1153e-4	2.6086e-4	2.14
$\boldsymbol{u}_h$	10^{-3}	10^2	7.9561e-3	1.8599e-3	8.0257e-4	4.4301e-4	2.7966e-4	2.07
		10^3	7.4971e-3	1.7544e-3	7.6102e-4	4.2264e-4	2.6831e-4	2.06
		10^4	7.4795e-3	1.7192e-3	7.4442e-4	4.1324e-4	2.6237e-4	2.07
		10^5	8.8961e-3	1.7613e-3	7.4460e-4	4.1147e-4	2.6085e-4	2.14
$\boldsymbol{u}_h$	10^{-4}	10^2	7.9685e-3	1.8716e-3	8.1251e-4	4.5112e-4	2.8617e-4	2.06
		10^3	7.4980e-3	1.7550e-3	7.6152e-4	4.2310e-4	2.6875e-4	2.06
		10^4	7.4791e-3	1.7192e-3	7.4445e-4	4.1327e-4	2.6239e-4	2.07
		10^5	8.8955e-3	1.7611e-3	7.4457e-4	4.1146e-4	2.6085e-4	2.14
p_h	10^{-2}	10^2	3.6430e-3	9.5152e-4	4.5788e-4	2.7916e-4	1.9248e-4	1.78
		10^3	5.9406e-3	1.3442e-3	5.8378e-4	3.3392e-4	2.2065e-4	2.00
		10^4	7.0683e-2	2.2240e-3	1.3530e-3	7.1754e-4	4.2669e-4	2.69
		10^5	4.9228e+0	2.7612e-1	3.3948e-2	6.1624e-3	1.5979e-3	5.33
p_h	10^{-3}	10^2	3.5251e-3	8.5488e-4	3.8281e-4	2.1957e-4	1.4404e-4	1.96
		10^3	6.0700e-3	1.3255e-3	5.5430e-4	3.0473e-4	1.9354e-4	2.11
		10^4	6.8462e-2	2.6044e-3	1.5157e-3	7.8883e-4	4.5951e-4	2.69
		10^5	4.9156e+0	2.7142e-1	3.1402e-2	4.4906e-3	2.4669e-4	7.32
p_h	10^{-4}	10^2	3.5111e-3	8.3979e-4	3.6855e-4	2.0655e-4	1.3225e-4	2.03
		10^3	6.0834e-3	1.3234e-3	5.5093e-4	3.0115e-4	1.8995e-4	2.13
		10^4	6.8244e-2	2.6558e-3	1.5363e-3	7.9862e-4	4.6466e-4	2.68
		10^5	4.9148e+0	2.7096e-1	3.1162e-2	4.3503e-3	1.8956e-4	7.60

Table 8. H^1 relative errors of $\boldsymbol{u}_h$ and p_h produced by the Bochev-Gunzburger-Lehoucq stabilized FEM (20) using P_1-P_1 finite elements for Example 1 with various viscosity ν and reaction coefficient σ, where we take $\delta = 0.05$ in (23).

H^1 error	ν	σ	$h^* = 1/20$	$1/40$	$1/60$	$1/80$	$1/100$	order
$\boldsymbol{u}_h$	10^{-2}	10^2	1.4249e-1	7.0283e-2	4.6601e-2	3.4849e-2	2.7829e-2	1.01
		10^3	1.4147e-1	7.0043e-2	4.6528e-2	3.4826e-2	2.7822e-2	1.01
		10^4	1.4052e-1	6.9777e-2	4.6391e-2	3.4744e-2	2.7771e-2	1.01
		10^5	1.3981e-1	6.9596e-2	4.6311e-2	3.4694e-2	2.7735e-2	1.00
$\boldsymbol{u}_h$	10^{-3}	10^2	1.4324e-1	7.0898e-2	4.7059e-2	3.5189e-2	2.8087e-2	1.01
		10^3	1.4156e-1	7.0126e-2	4.6611e-2	3.4906e-2	2.7898e-2	1.01
		10^4	1.4054e-1	6.9788e-2	4.6400e-2	3.4753e-2	2.7780e-2	1.01
		10^5	1.3982e-1	6.9599e-2	4.6313e-2	3.4695e-2	2.7736e-2	1.00
$\boldsymbol{u}_h$	10^{-4}	10^2	1.4334e-1	7.1042e-2	4.7228e-2	3.5366e-2	2.8261e-2	1.01
		10^3	1.4157e-1	7.0136e-2	4.6622e-2	3.4918e-2	2.7912e-2	1.01
		10^4	1.4054e-1	6.9789e-2	4.6401e-2	3.4754e-2	2.7781e-2	1.01
		10^5	1.3982e-1	6.9599e-2	4.6313e-2	3.4696e-2	2.7736e-2	1.00
p_h	10^{-2}	10^2	8.0403e-2	4.1180e-2	2.8426e-2	2.2137e-2	1.8386e-2	0.90
		10^3	8.4342e-2	4.5200e-2	3.0908e-2	2.3746e-2	1.9487e-2	0.91
		10^4	2.2742e-1	3.9764e-2	3.4014e-2	2.7873e-2	2.3290e-2	1.10
		10^5	8.5961e+0	7.3717e-1	1.3700e-1	3.5321e-2	1.4398e-2	4.11
p_h	10^{-3}	10^2	7.9687e-2	3.9673e-2	2.6550e-2	2.0061e-2	1.6200e-2	0.98
		10^3	8.4605e-2	4.4822e-2	3.0151e-2	2.2709e-2	1.8237e-2	0.97
		10^4	2.2241e-1	4.0260e-2	3.4228e-2	2.7864e-2	2.3125e-2	1.10
		10^5	8.5782e+0	7.2564e-1	1.3188e-1	3.2910e-2	1.3859e-2	4.12
p_h	10^{-4}	10^2	7.9597e-2	3.9438e-2	2.6207e-2	1.9638e-2	1.5716e-2	1.01
		10^3	8.4631e-2	4.4780e-2	3.0065e-2	2.2583e-2	1.8075e-2	0.97
		10^4	2.2192e-1	4.0316e-2	3.4251e-2	2.7862e-2	2.3107e-2	1.10
		10^5	8.5764e+0	7.2450e-1	1.3140e-1	3.2708e-2	1.3853e-2	4.11

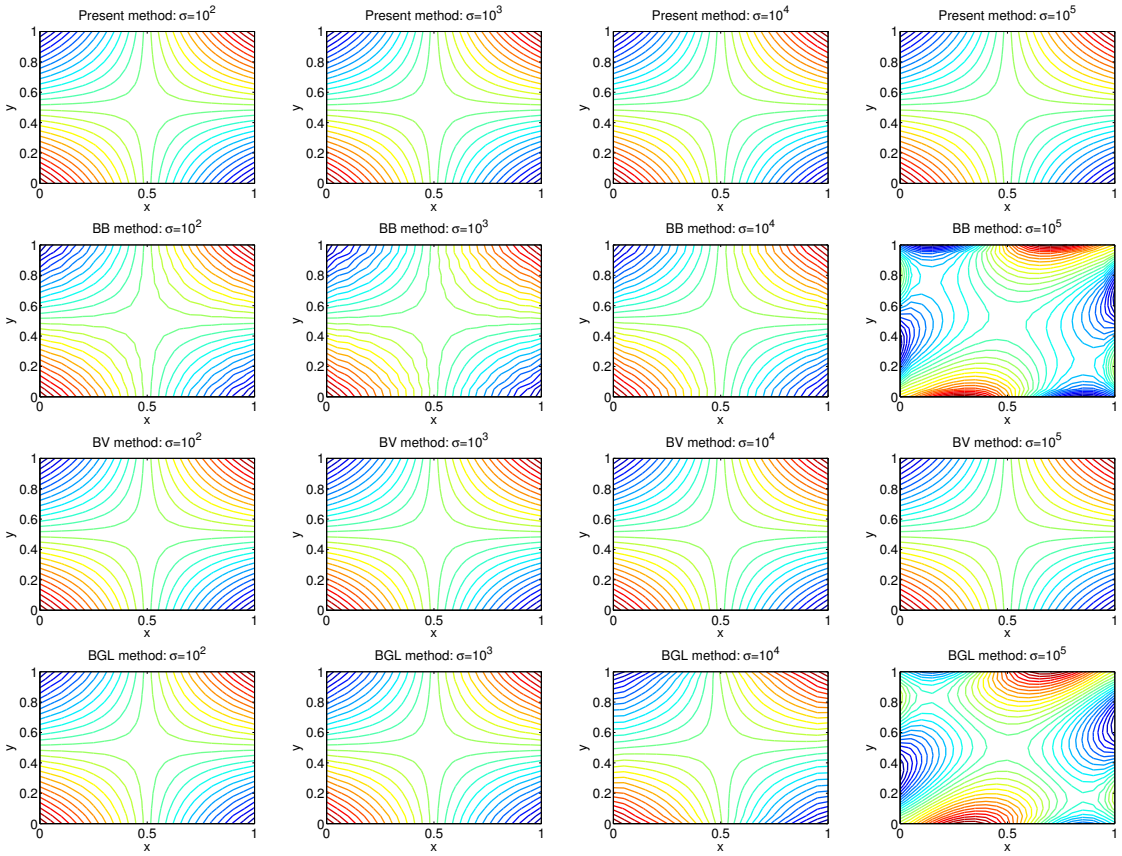

Figure 1. Contours of P_1 pressure approximations produced by various stabilized FEMs on a uniform triangular mesh with $h^* = 1/20$ for Example 1, where $\nu = 10^{-3}$ and $\sigma = 10^m$ for $m = 2, 3, 4, 5$.

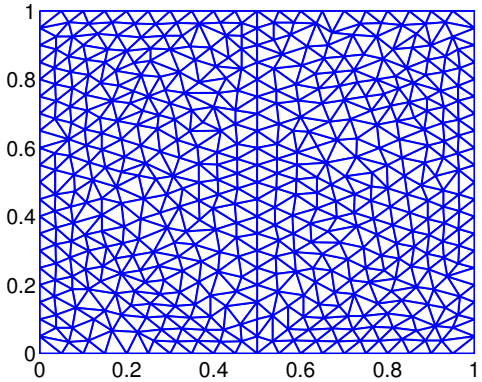

Figure 2. An unstructured triangular mesh with $h^* = 1/20$.

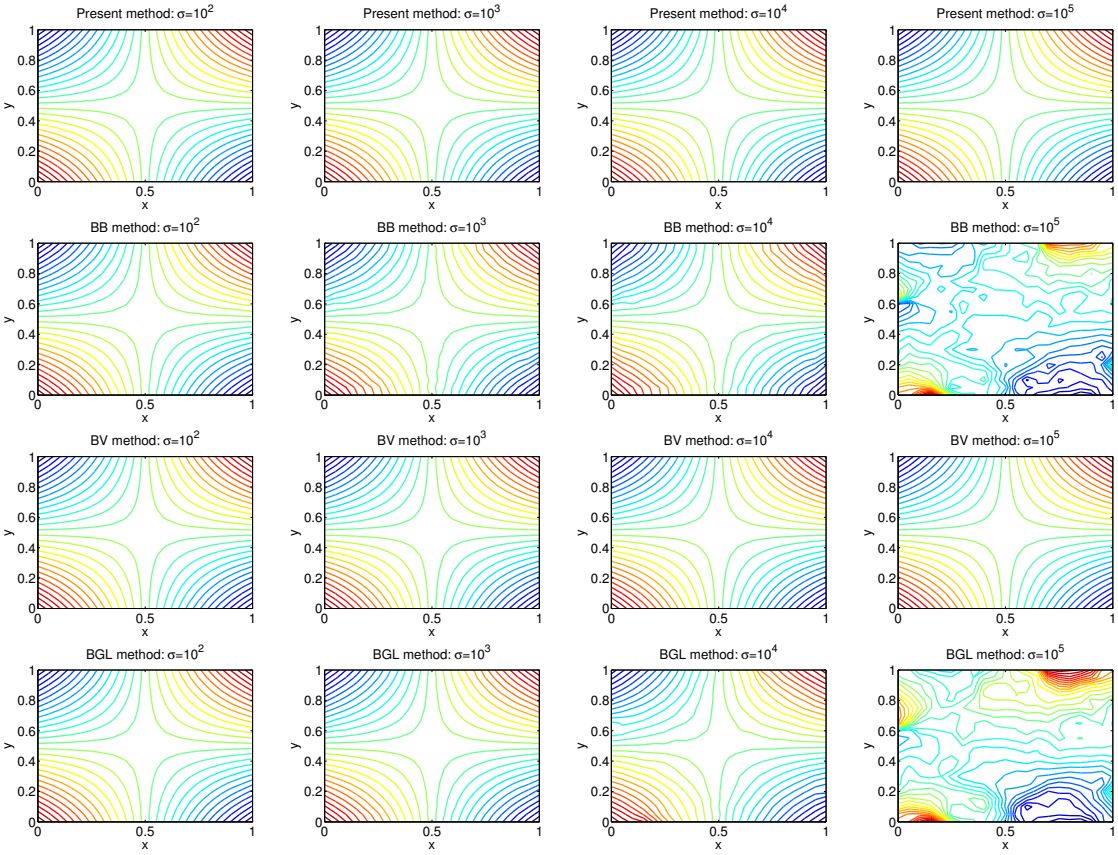

Figure 3. Contours of P_1 pressure approximations produced by various stabilized FEMs on an unstructured triangular mesh with $h^* = 1/20$ for Example 1, where $\nu = 10^{-3}$ and $\sigma = 10^m$ for $m = 2, 3, 4, 5$.

Table 9. L^2 relative errors of $\boldsymbol{u}_h$ and p_h produced by the proposed stabilized FEM (5) with new stabilization parameters given in Remark 6 and using P_2-P_2 finite elements for Example 1 with various viscosity ν and reaction coefficient σ.

L^2 error	ν	σ	h^* = 1/20	1/40	1/60	1/80	1/100	order
$\boldsymbol{u}_h$	10^{-2}	10^2	9.4692e-4	1.1085e-4	2.7520e-5	9.9262e-6	4.4804e-6	3.41
		10^3	3.8520e-4	5.9588e-5	1.8569e-5	7.6618e-6	3.7458e-6	2.96
		10^4	3.0629e-4	3.9170e-5	1.1832e-5	5.0837e-6	2.6429e-6	2.95
		10^5	3.0413e-4	3.8400e-5	1.1405e-5	4.8169e-6	2.4683e-6	2.99
$\boldsymbol{u}_h$	10^{-3}	10^2	1.4338e-3	2.8902e-4	9.9812e-5	4.3261e-5	2.1534e-5	2.74
		10^3	3.9789e-4	7.3201e-5	2.8667e-5	1.4615e-5	8.4921e-6	2.38
		10^4	3.0630e-4	3.9222e-5	1.1911e-5	5.1781e-6	2.7437e-6	2.91
		10^5	3.0413e-4	3.8400e-5	1.1405e-5	4.8170e-6	2.4684e-6	2.99
$\boldsymbol{u}_h$	10^{-4}	10^2	1.5252e-3	3.6341e-4	1.5454e-4	8.2463e-5	4.9626e-5	2.16
		10^3	3.9935e-4	7.5310e-5	3.0868e-5	1.6729e-5	1.0450e-5	2.21
		10^4	3.0630e-4	3.9228e-5	1.1921e-5	5.1903e-6	2.7585e-6	2.91
		10^5	3.0413e-4	3.8400e-5	1.1405e-5	4.8170e-6	2.4684e-6	2.99
p_h	10^{-2}	10^2	6.8153e-5	1.2327e-5	4.2006e-6	1.9737e-6	1.1261e-6	2.57
		10^3	5.6732e-5	1.3429e-5	4.8216e-6	2.2373e-6	1.2410e-6	2.48
		10^4	3.5619e-5	9.4945e-6	4.2398e-6	2.3070e-6	1.3993e-6	2.06
		10^5	3.2941e-5	8.3672e-6	3.7302e-6	2.0944e-6	1.3328e-6	2.00
p_h	10^{-3}	10^2	2.0044e-5	8.5588e-6	4.7962e-6	2.8754e-6	1.8012e-6	1.63
		10^3	7.3820e-6	2.9967e-6	1.7227e-6	1.1271e-6	7.8846e-7	1.44
		10^4	3.6352e-6	1.0378e-6	5.1707e-7	3.2105e-7	2.2333e-7	1.70
		10^5	3.3001e-6	8.4290e-7	3.7933e-7	2.1579e-7	1.3961e-7	1.96
p_h	10^{-4}	10^2	2.4374e-6	1.4520e-6	1.1811e-6	1.0241e-6	8.9359e-7	0.59
		10^3	7.6179e-7	3.4101e-7	2.2616e-7	1.7528e-7	1.4718e-7	0.96
		10^4	3.6429e-7	1.0482e-7	5.3006e-8	3.3645e-8	2.4091e-8	1.64
		10^5	3.3007e-7	8.4353e-8	3.7998e-8	2.1648e-8	1.4031e-8	1.96

Table 10. H^1 relative errors of $\boldsymbol{u}_h$ and p_h produced by the proposed stabilized FEM (5) with new stabilization parameters given in Remark 6 and using P_2-P_2 finite elements for Example 1 with various viscosity ν and reaction coefficient σ.

H^1 error	ν	σ	$h^* = 1/20$	$1/40$	$1/60$	$1/80$	$1/100$	order
$\boldsymbol{u}_h$	10^{-2}	10^2	1.7633e-2	4.2320e-3	1.6024e-3	7.8450e-4	4.5086e-4	2.35
		10^3	8.4195e-3	2.5229e-3	1.1765e-3	6.5096e-4	4.0123e-4	1.96
		10^4	7.2907e-3	1.8475e-3	8.3219e-4	4.7437e-4	3.0707e-4	1.96
		10^5	7.2700e-3	1.8255e-3	8.1215e-4	4.5709e-4	2.9267e-4	2.00
$\boldsymbol{u}_h$	10^{-3}	10^2	2.7077e-2	1.1251e-2	5.8745e-3	3.4048e-3	2.1212e-3	1.72
		10^3	8.6306e-3	3.0273e-3	1.7537e-3	1.1864e-3	8.6003e-4	1.41
		10^4	7.2908e-3	1.8492e-3	8.3617e-4	4.8082e-4	3.1579e-4	1.94
		10^5	7.2700e-3	1.8255e-3	8.1215e-4	4.5710e-4	2.9269e-4	2.00
$\boldsymbol{u}_h$	10^{-4}	10^2	2.8886e-2	1.4241e-2	9.1776e-3	6.5602e-3	4.9476e-3	1.13
		10^3	8.6551e-3	3.1072e-3	1.8831e-3	1.3544e-3	1.0558e-3	1.24
		10^4	7.2908e-3	1.8494e-3	8.3663e-4	4.8166e-4	3.1709e-4	1.93
		10^5	7.2700e-3	1.8255e-3	8.1215e-4	4.5710e-4	2.9269e-4	2.00
p_h	10^{-2}	10^2	5.1157e-4	2.9735e-4	2.1264e-4	1.6491e-4	1.3433e-4	0.85
		10^3	6.2157e-4	3.2211e-4	2.1964e-4	1.6734e-4	1.3531e-4	0.95
		10^4	6.6167e-4	3.4092e-4	2.2877e-4	1.7208e-4	1.3793e-4	0.98
		10^5	6.6603e-4	3.4413e-4	2.3102e-4	1.7370e-4	1.3913e-4	0.98
p_h	10^{-3}	10^2	6.2239e-5	3.6364e-5	2.4296e-5	1.7634e-5	1.3716e-5	1.00
		10^3	6.2189e-5	3.1916e-5	2.1620e-5	1.6417e-5	1.3250e-5	0.96
		10^4	6.6193e-5	3.4089e-5	2.2860e-5	1.7182e-5	1.3761e-5	0.98
		10^5	6.6608e-5	3.4416e-5	2.3103e-5	1.7371e-5	1.3913e-5	0.98
p_h	10^{-4}	10^2	6.8364e-6	5.0213e-6	4.2581e-6	3.7151e-6	3.2564e-6	0.48
		10^3	6.2212e-6	3.1977e-6	2.1807e-6	1.6779e-6	1.3796e-6	0.92
		10^4	6.6196e-6	3.4089e-6	2.2858e-6	1.7179e-6	1.3758e-6	0.98
		10^5	6.6609e-6	3.4416e-6	2.3103e-6	1.7371e-6	1.3913e-6	0.98

Example 2. (Q_1-Q_1 *finite elements*) This example is taken from [30] with a slight modification to keep $\int_\Omega p = 0$. We consider problem (1) on the unit square domain $\Omega = (0,1) \times (0,1)$ with the following smooth exact solution:

$$\begin{aligned} u_1(x,y) &= 100x^2(1-x)^2(2y - 6y^2 + 4y^3), \\ u_2(x,y) &= -u_1(y,x), \\ p(x,y) &= 100(x - x^2) - \frac{100}{6}. \end{aligned}$$

Then $\boldsymbol{u} = \boldsymbol{0}$ on $\partial\Omega$ and $\int_\Omega p = 0$. In this example, we verify the convergence behavior of various stabilized FEMs using Q_1-Q_1 finite elements. It is no surprise that we reach conclusions similar to those obtained in Example 1. In summary, by examining the accuracy and stability, we find that the present stabilized FEM and the Barrenechea-Valentin method can achieve better convergence behavior than the Barrenechea-Blasco method and the Bochev-Gunzburger-Lehoucq method when $0 < \nu \ll 1$ and $\sigma \gg 1$. In Figure 4, we display the contour plots of Q_1 pressure approximations produced by various stabilized FEMs on a uniform square mesh with $h^* = 1/20$ for $\nu = 10^{-3}$ and $\sigma = 10^m$, $m = 2, 3, 4, 5$. Again, we may observe that the pressure instabilities appear in the Barrenechea-Blasco method and the Bochev-Gunzburger-Lehoucq method when the reaction coefficient σ is sufficiently large.

Example 3. (P_1-P_1 *finite elements*) We study another example that is tested in [1]. Consider the generalized Stokes system (1) on the domain $\Omega = (0,1) \times (0,1)$ with the following smooth exact solution:

$$\begin{aligned} u_1(x,y) &= 2\pi x^2(1-x)^2 \cos(\pi y)\sin(\pi y), \\ u_2(x,y) &= 2(1-x)(2x^2 - x)\sin^2(\pi y), \\ p(x,y) &= \sin(x)\cos(y) + (\cos(1) - 1)\sin(1). \end{aligned}$$

One can check that $\boldsymbol{u} = \boldsymbol{0}$ on $\partial\Omega$ and $\int_\Omega p = 0$. We perform the numerical simulations using P_1-P_1 finite elements on the uniform triangular meshes as that described in Example 1. Once again, we find that the pressure instabilities appear in the Barrenechea-Blasco and the Bochev-Gunzburger-Lehoucq methods when the reaction coefficient σ is large enough; see Figure 5.

Example 4. (*The lid-driven cavity problem using P_1-P_1 finite elements*) Let $I = (0, T)$ denote the time interval under consideration and $\Omega = (0,1) \times (0,1)$ the given spatial domain. In this example, we first study the time-dependent lid-driven cavity problem governed by the following time-dependent, incompressible Stokes equations (cf. [30]):

$$\begin{cases} \dfrac{\partial \boldsymbol{u}}{\partial t} - \nu\Delta\boldsymbol{u} + \nabla p = \boldsymbol{f} & \text{in } I \times \Omega, \\ \nabla \cdot \boldsymbol{u} = 0 & \text{in } I \times \Omega, \\ \boldsymbol{u} = \boldsymbol{0} & \text{on } \overline{I} \times (\partial\Omega \setminus ([0,1] \times \{1\})), \\ \boldsymbol{u} = (1,0)^\top & \text{on } \overline{I} \times ([0,1] \times \{1\}), \\ \boldsymbol{u} = \boldsymbol{u}_0 & \text{on } \{0\} \times \Omega, \end{cases} \tag{60}$$

where we set the source function $\boldsymbol{f} = \boldsymbol{0}$ in $I \times \Omega$ and the initial condition $\boldsymbol{u}_0 = \boldsymbol{0}$ in $\{0\} \times \Omega$. See Figure 6 for the statement of the boundary conditions.

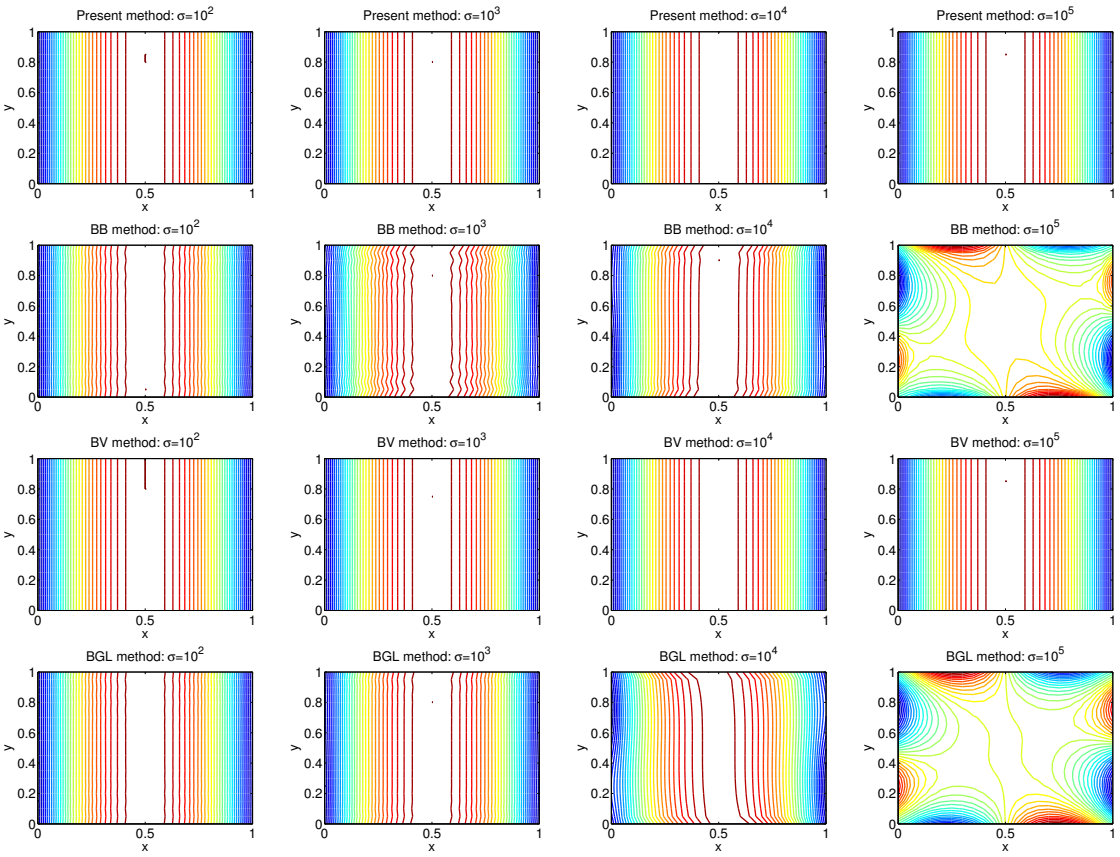

Figure 4. Contours of Q_1 pressure approximations produced by various stabilized FEMs on a uniform square mesh with $h^* = 1/20$ for Example 2, where $\nu = 10^{-3}$ and $\sigma = 10^m$ for $m = 2, 3, 4, 5$.

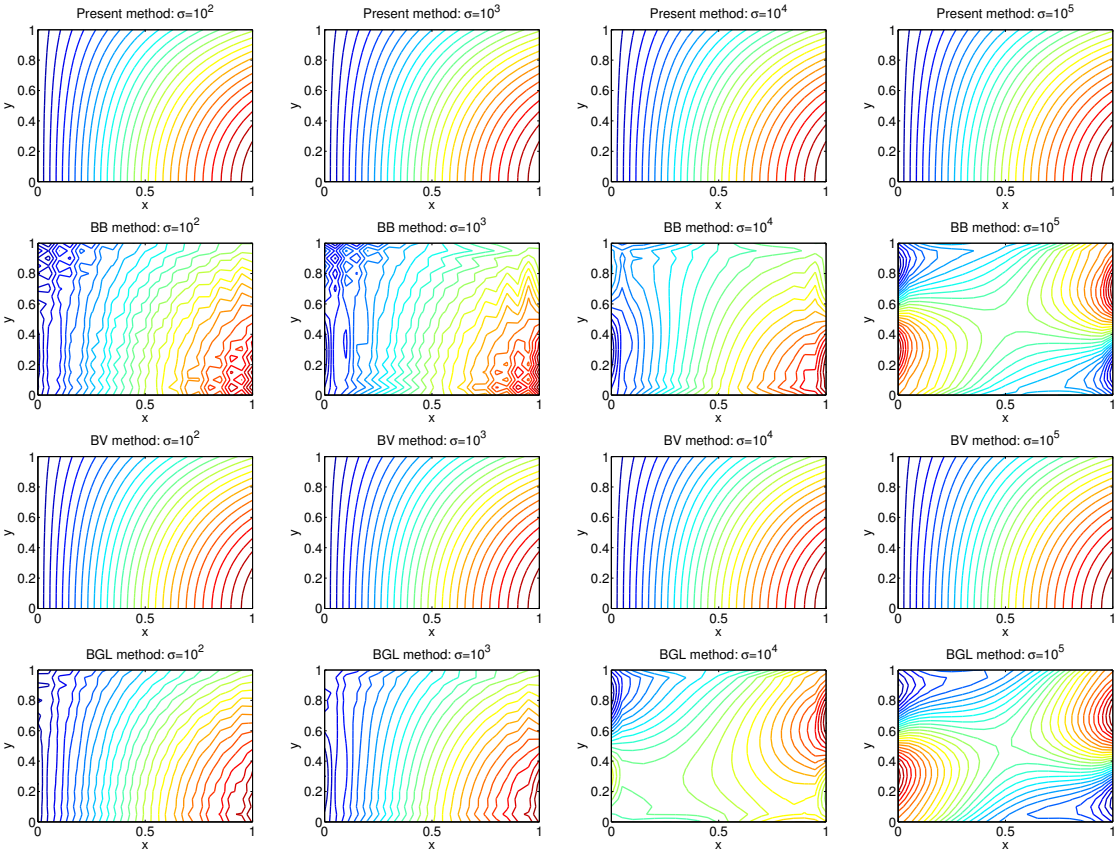

Figure 5. Contours of P_1 pressure approximations produced by various stabilized FEMs on a uniform triangular mesh with $h^* = 1/20$ for Example 3, where $\nu = 10^{-3}$ and $\sigma = 10^m$ for $m = 2, 3, 4, 5$.

Let $0 = t_0 < t_1 < \cdots < t_{\ell-1} < t_\ell = T$ be a a subdivision of the time interval $(0, T)$ with a constant time step $\delta t = t_n - t_{n-1}$ for $n = 1, 2, \cdots, \ell$. Then we set $\sigma = 1/\delta t$. For any $n \geq 1$, the unknowns $\boldsymbol{u}_h^n$ and p_h^n at time step n are computed by induction, using values at the previous time step. The time discretization is performed by using, for example, the first-order backward Euler scheme and the spatial discretization is carried out by employing, for example, the newly proposed stabilized FEM (5), then we have the following fully discrete problem at time step n:

$$\begin{aligned}
&\sigma(\boldsymbol{u}_h^n, \boldsymbol{v}_h)_0 + \nu(\nabla \boldsymbol{u}_h^n, \nabla \boldsymbol{v}_h)_0 - (p_h^n, \nabla \cdot \boldsymbol{v}_h)_0 - (\nabla \cdot \boldsymbol{u}_h^n, q_h)_0 \\
&- \sum_{K \in \mathcal{T}_h} \frac{h^2}{\sigma h^2 + 12\nu} (\sigma \boldsymbol{u}_h^n - \nu \Delta \boldsymbol{u}_h^n + \nabla p_h^n, \sigma \boldsymbol{v}_h - \nu \Delta \boldsymbol{v}_h + \nabla q_h)_{0,K} + \sum_{K \in \mathcal{T}_h} \frac{12\nu}{\sigma h^2 + 12\nu} (\nabla \cdot \boldsymbol{u}_h^n, \nabla \cdot \boldsymbol{v}_h)_{0,K} \\
&= (\boldsymbol{f}^n + \sigma \boldsymbol{u}_h^{n-1}, \boldsymbol{v}_h)_0 - \sum_{K \in \mathcal{T}_h} \frac{h^2}{\sigma h^2 + 12\nu} (\boldsymbol{f}^n + \sigma \boldsymbol{u}_h^{n-1}, \sigma \boldsymbol{v}_h - \nu \Delta \boldsymbol{v}_h + \nabla q_h)_{0,K} \quad \forall\, (\boldsymbol{v}_h, q_h) \in \mathcal{V}_h \times \mathcal{Q}_h, \qquad (61)
\end{aligned}$$

where $\boldsymbol{u}_h^n$ is required to satisfy the prescribed boundary conditions. In the following simulations, we will consider various stabilized FEMs with P_1-P_1 finite elements on a uniform triangular mesh, as that described in Example 1.

We first consider the case of $\nu = 10^{-4}$, $\delta t = 10^{-4}$ and $h^* = 1/40$. In such case, we have $\delta t \ll h = \sqrt{2} h^*$ and $\nu \ll \sigma h^2 = 12.5$. The pressure contours at the first, 5th, 10th and the 100th time steps produced by various stabilized FEMs are depicted in Figure 7. From Figure 7, we may observe that all methods display comparable results at the first time step. However, we also find that a large instability occurs at the regions near two top corners in both the Barrenechea-Blasco method (12) and the Bochev-Gunzburger-Lehoucq method (20) as the time evolves, while the other two methods still retain high robustness.

Next, we study the case of $\nu = 10^{-2}$, $\delta t = 2/100$ and $h^* = 1/100$. Notice that in this case, we have $\delta t > h = \sqrt{2} h^*$ and $\nu = \sigma h^2 = 10^{-2}$. The pressure contours are depicted in Figure 8. Again, we find that the proposed stabilized FEM (5) and the Barrenechea-Valentin method (16) still retain their high stability as the time evolves. However, the stability of the pressure approximations produced by the other two stabilization methods are completely lost.

We now perform the simulations of the present stabilized FEM (5) and the Barrenechea-Valentin method (16) to reach a steady state. The stopping criterion for the time advancing is given by

$$\frac{\|\boldsymbol{u}_h^n - \boldsymbol{u}_h^{n-1}\|_0}{\|\boldsymbol{u}_h^n\|_0} < 10^{-5}.$$

The contours of stream function and pressure at the steady state are depicted in Figure 9 and Figure 10, where the time T reaching the steady state is also indicated in each figure. As we have seen before, these two stabilized FEMs show a very similar behavior.

Finally, we consider a time-independent lid-driven cavity problem. We solve the generalized Stokes equations (1), but with the boundary condition described in Figure 6, using P_1-P_1 finite elements on a uniform triangular mesh of mesh size $h^* = 1/20$. In Figure 11, we show a vertical cross section of the velocity component u_1 of the lid-driven cavity problem with $\nu = 10^{-3}$ and $\sigma = 10^3$, comparing the solutions of the present method (5) and the Barrenechea-Valentin method (16). One can observe the presence of a boundary layer on the velocity that is well recovered by both stabilization methods, even we use a rather coarse mesh.

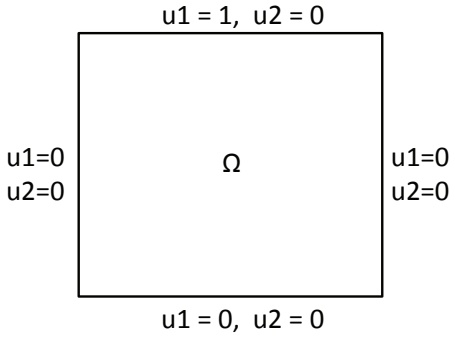

Figure 6. Statement of the boundary conditions of the lid-driven cavity problem for $t \in [0, T]$.

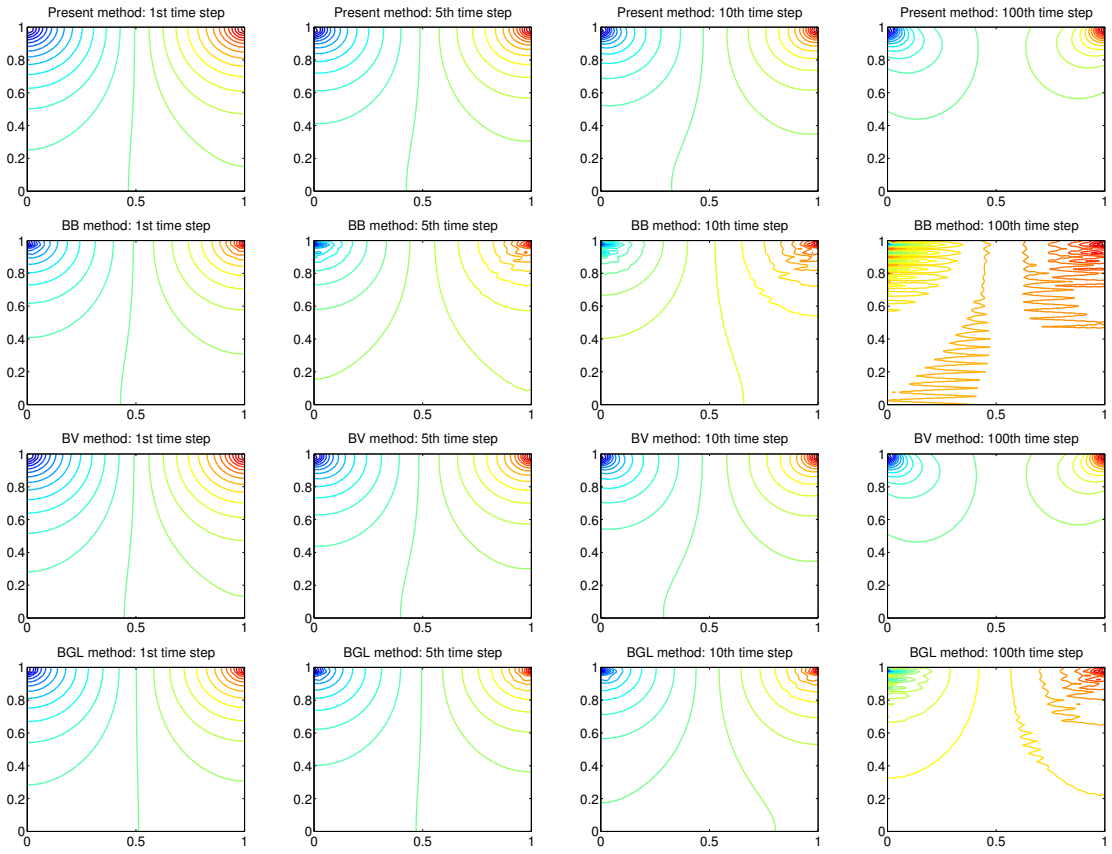

Figure 7. Contours of P_1 pressure approximations at the first, 5th, 10th and 100th time steps produced by various stabilized FEMs on a uniform triangular mesh with $h^* = 1/40$ for the time-dependent lid-driven cavity problem, where $\nu = 10^{-4}$ and $\delta t = 10^{-4}$ ($\sigma = 10^4$).

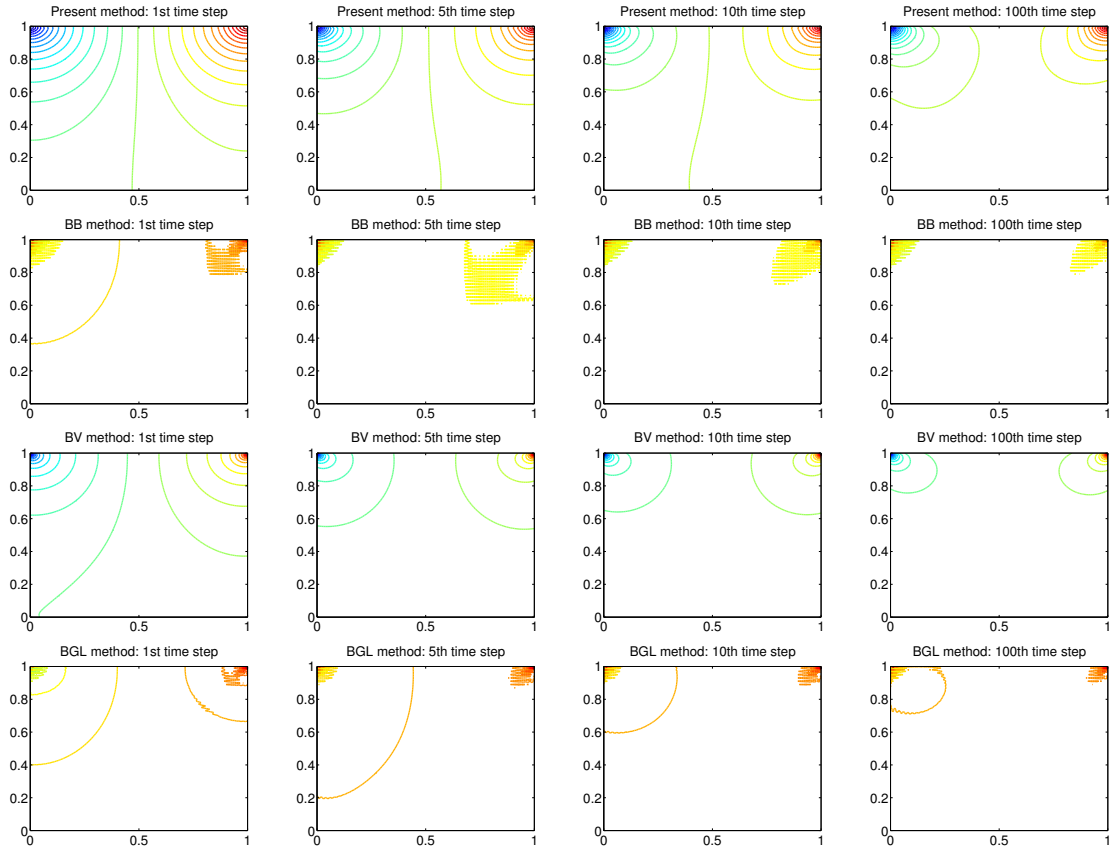

Figure 8. Contours of P_1 pressure approximations at the first, 5th, 10th and 100th time steps produced by various stabilized FEMs on a uniform triangular mesh with $h^* = 1/100$ for the time-dependent lid-driven cavity problem, where $\nu = 10^{-2}$ and $\delta t = 2/100$ ($\sigma = 50$).

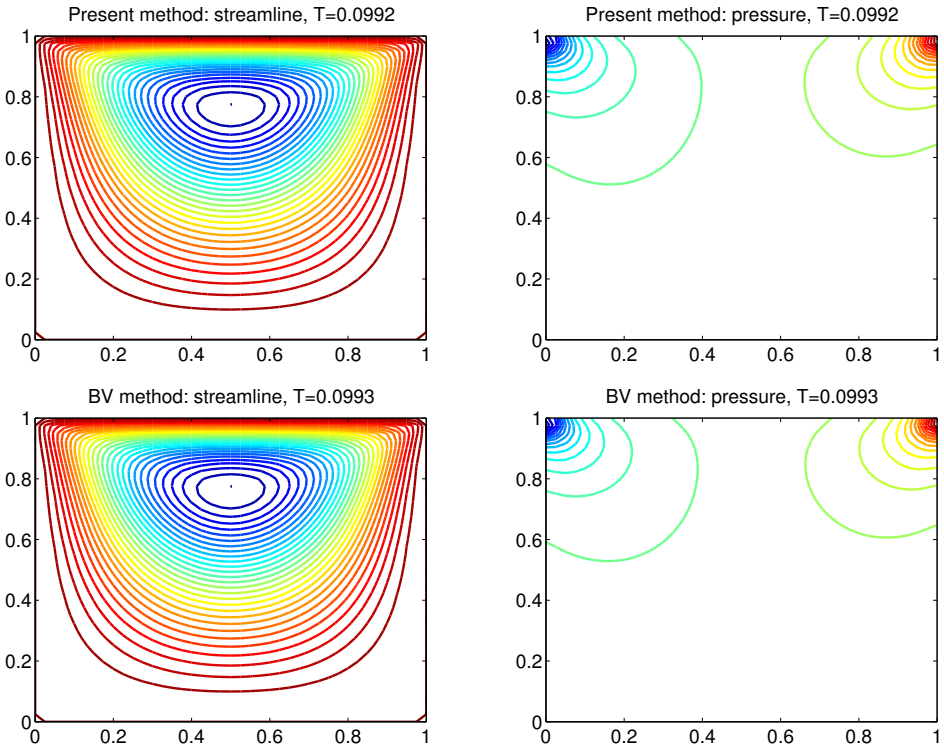

Figure 9. Contours of stream function and pressure at the steady state produced by the present stabilized FEM and the Barrenechea-Valentin method on a uniform triangular mesh with $h^* = 1/40$ for the time-dependent lid-driven cavity problem, where $\nu = 10^{-4}$ and $\delta t = 10^{-4}$ ($\sigma = 10^4$).

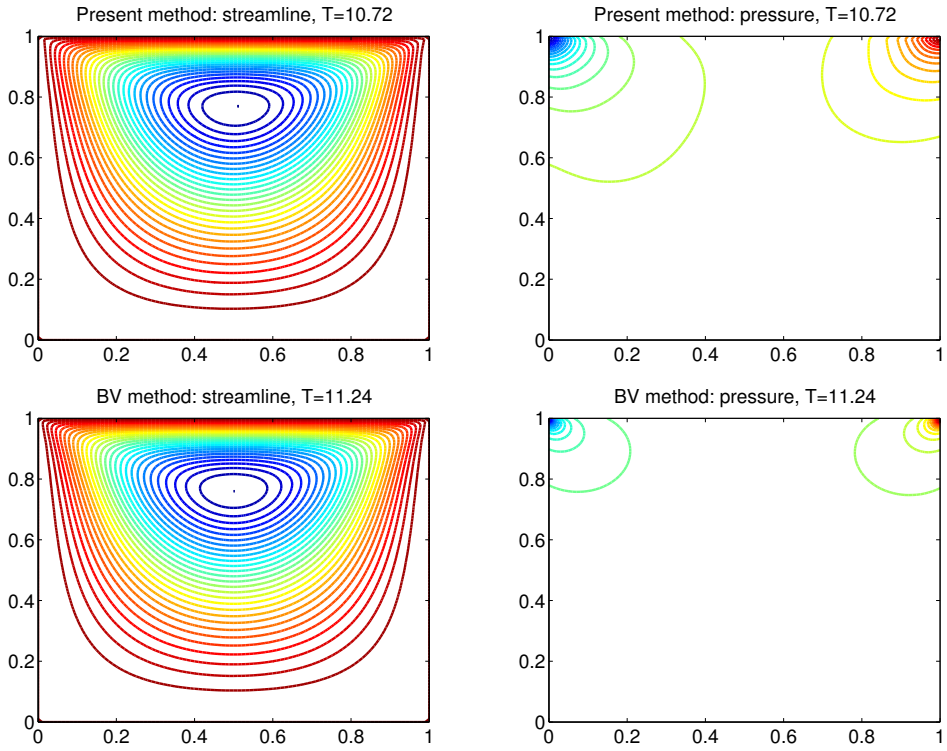

Figure 10. Contours of stream function and pressure at the steady state produced by the present stabilized FEM and the Barrenechea-Valentin method on a uniform triangular mesh with $h^* = 1/100$ for the time-dependent lid-driven cavity problem, where $\nu = 10^{-2}$ and $\delta t = 2/100$ ($\sigma = 50$).

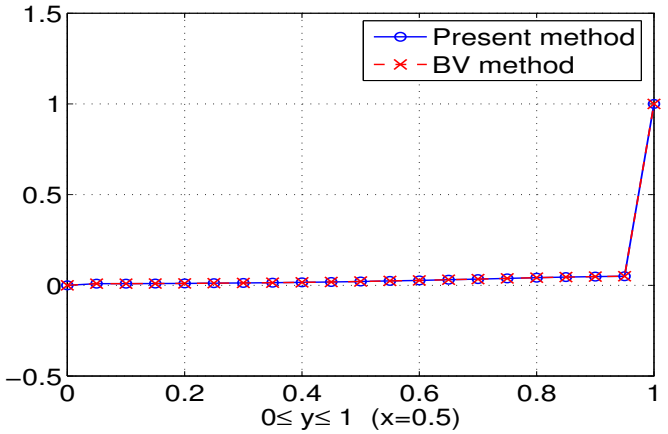

Figure 11. Vertical cross section of the velocity component u_1 at $x = 0.5$ of the time-independent lid-driven cavity problem with $\nu = 10^{-3}$ and $\sigma = 10^3$.

5. Summary and conclusions

In this paper, we have proposed a novel stabilized FEM for the generalized Stokes system with a small viscosity and a large reaction coefficient. This system arises from the time-discretization of transient Stokes problem with a small time step, as discretized in practical problems of fast reaction. The unstable and inaccurate finite element pressure solutions may be caused when the finite element inf-sup stabilization is applied to solve the system. More precisely, when the magnitude of the viscosity, the reaction coefficient, and the mesh size are not balanced suitably, pressure instability and less accuracy would happen. The proposed stabilized FEM employs the C^0 piecewise P_1 (or Q_1) elements for both velocity field and pressure on the same mesh and uses the residuals of the momentum equation and the divergence-free equation to define the stabilization terms, in which the stabilization parameters are fixed and element-independent, without a comparison of the viscosity, the reaction coefficient and the mesh size.

We have used the finite element solution of an auxiliary boundary value problem as the interpolating function for velocity and the H^1-seminorm projection for pressure, instead of the usual nodal interpolants, to derive the error estimates of the stabilized finite element solutions in the L^2 and H^1 norms. Moreover, we have explicitly established the dependence of error bounds on the viscosity, the reaction coefficient and the mesh size. Based on the error analysis, we have found that the proposed stabilized FEM is particularly suitable for generalized Stokes systems with a small viscosity and a large reaction coefficient. To the best of our knowledge, it has never been achieved before in the error analysis of other stabilization methods in the literature. We have also compared numerically the effectiveness of the proposed method with three existing stabilization methods, including the Barrenechea-Blasco stabilized FEM [30], the Barrenechea-Valentin stabilized FEM [17], and the Bochev-Gunzburger-Lehoucq stabilized FEM [1]. We have found that in addition to its theoretical suitability for problems with a small viscosity and a large reaction coefficient, the proposed stabilized FEM can achieve better accuracy and stability when compared with the Barrenechea-Blasco and the Bochev-Gunzburger-Lehoucq methods, while it is comparable with the Barrenechea-Valentin method in the case of $\sigma h^2 \gg \nu$ and $\nu \ll 1$.

Finally, we conclude this paper with the following two remarks:

- By a close inspection, one can find that the Barrenechea-Valentin stabilized FEM (16) is essentially similar to the newly proposed stabilized FEM (5) when $\sigma h^2 \gg \nu$ and $\nu \ll 1$, except it does not contain the divergence-free stabilization term and its stabilization parameter is element-dependent. The numerical results reported in Section 4 also show that these two methods exhibit a very similar convergence behavior. Unfortunately, in [17], the authors did not give sharp error estimates with respect to ν and σ. We believe that using the same techniques developed in this paper with some additional assumption on the triangulations, such as the quasi-uniformity [4, 7, 38], one can improve largely the error estimates given in [17].

- In our recent work [40], we have provided some sharp error estimates for the scalar reaction-convection-diffusion equation with a small diffusivity and a large reaction coefficient. Combining the results derived in

[40] with the similar idea given in this paper, one may give some sharp error estimates of the incompressible Oseen-type problem for $0 < \nu \ll 1$ and $\sigma \gg 1$, where finite element stabilization serves the dual purpose of avoiding the inf-sup condition and providing the upwinding necessary for the convection terms.

For these two issues, the efforts are in progress and we will report the results in the near future.

Acknowledgments. The work of H.-Y. Duan was partially supported by the National Natural Science Foundation of China under the grants 11071132 and 11171168 and the Research Fund for the Doctoral Program of Higher Education of China under grants 20100031110002 and 20120031110026. The work of P.-W. Hsieh and S.-Y. Yang was partially supported by the National Science Council of Taiwan under the grants NSC 102-2115-M-033-007-MY2 and NSC 101-2115-M-008-008-MY2.

References

[1] P. B. Bochev, M. D. Gunzburger, and R. B. Lehoucq, On stabilized finite element methods for the Stokes problem in the small time step limit, *Int. J. Numer. Meth. Fluids,* 53 (2007), pp. 573-597.
[2] P. B. Bochev, M. D. Gunzburger, and J. N. Shadid, On inf-sup stabilized finite element methods for transient problems, *Comput. Methods Appl. Mech. Engrg.,* 193 (2004), pp. 1471-1489.
[3] I. Harari, Stability of semidiscrete formulations for parabolic problems at small time steps, *Comput. Methods Appl. Mech. Engrg.,* 193 (2004), pp. 1491-1516.
[4] C. Johnson, *Numerical Solution of Partial Differential Equations by the Finite Element Method,* Cambridge University Press, Cambridge, 1987.
[5] V. Thomée, *Galerkin Finite Element Methods for Parabolic Problems, Second Edition,* Springer-Verlag, Berlin, 2006.
[6] P. B. Bochev and M. D. Gunzburger, *Least-Squares Finite Element Methods,* Applied Mathematical Sciences, Vol. 166, Springer, New York, 2009.
[7] S. C. Brenner and L. R. Scott, *The Mathematical Theory of Finite Element Methods*, Springer-Verlag, New York, 1994.
[8] F. Brezzi and M. Fortin, *Mixed and Hybrid Finite Element Methods,* Springer-Verlag, New York, 1991.
[9] V. Girault and P. A. Raviart, *Finite Element Methods for Navier-Stokes Equations: Theory and Algorithms,* Springer-Verlag, New York, 1986.
[10] F. Brezzi and J. Douglas Jr., Stabilized mixed methods for the Stokes problem, *Numer. Math.,* 53 (1988), pp. 225-235.
[11] F. Brezzi and J. Pitkäranta, On the stabilization of finite element approximations of the Stokes problem, In: W. Hackbush, editor, *Efficient Solution of Elliptic Systems, Notes on Numerical Fluid Mechanics,* Vol. 10, pp. 11-19, Braunschweig, Vieweg, 1984.
[12] A. N. Brooks and T. J. R. Hughes, Streamline upwind/Petrov-Galerkin formulations for convective dominated flows with a particular emphasis on the incompressible Navier-Stokes equations, *Comput. Methods Appl. Mech. Engrg.,* 32 (1982), pp. 199-259.
[13] J. Douglas and J. Wang, An absolutely stabilized finite element method for the Stokes problem, *Math. Comput.,* 52 (1989), pp. 495-508.
[14] L. P. Franca, T. J. R. Hughes, and R. Stenberg, Stabilized finite element methods for the Stokes problem, In M. Gunzburger and R. A. Nicolaides, Eds., *Incompressible Computational Fluid Dynamics,* pp. 87-108, Cambridge University Press, 1993.
[15] T. J. R. Hughes and L. P. Franca, A new finite element formulation for computational fluid dynamics: VII. The Stokes problem with various well-posed boundary conditions: symmetric formulations that converge for all velocity/pressure spaces, *Comput. Methods Appl. Mech. Engrg.,* 65 (1987), pp. 85-96.
[16] T. J. R. Hughes, L. P. Franca, and M. Balestra, A new finite element formulation for computational fluids dynamics: V. Circumventing the Babuska-Brezzi condition: a stable Petrov-Galerkin formulation of the Stokes problem accommodating equal-order interpolations, *Comput. Methods Appl. Mech. Engrg.,* 59 (1986), pp. 85-99.
[17] G. R. Barrenechea and F. Valentin, An unusual stabilized finite element method for a generalized Stokes problem, *Numer. Math.,* 92 (2002), pp. 653-677.
[18] L. P. Franca and S. P. Oliveira, Pressure bubbles stabilization features in the Stokes problem, *Comput. Methods Appl. Mech. Engrg.,* 192 (2003), pp. 1929-1937.
[19] F. Brezzi, L. P. Franca, and A. Russo, Further considerations on residual-free bubbles for advective-diffusive equations, *Comput. Methods Appl. Mech. Engrg.,* 166 (1998), pp. 25-33.
[20] F. Brezzi and A. Russo, Choosing bubbles for advection-diffusion problems, *Math. Models Meth. Appl. Sci.,* 4 (1994), pp. 571-587.
[21] H.-Y. Duan, A new stabilized finite element method for solving the advection-diffusion equations, *J. Comput. Math.,* 20 (2002), pp. 57-64.
[22] L. P. Franca and C. Farhat, Bubble functions prompt unusual stabilized finite element methods, *Comput. Methods Appl. Mech. Engrg.,* 123 (1995), pp. 299-308.
[23] L. P. Franca, S. L. Frey, and T. J. R. Hughes, Stabilized finite element methods: I. application to the advective-diffusive model, *Comput. Methods Appl. Mech. Engrg.,* 95 (1992), pp. 253-276.
[24] L. P. Franca, G. Hauke, and A. Masud, Revisiting stabilized finite element methods for the advective-diffusive equation, *Comput. Methods Appl. Mech. Engrg.,* 195 (2006), pp. 1560-1572.

[25] L. P. Franca and F. Valentin, On an improved unusual stabilized finite element method for the advective-reactive-diffusive equation, *Comput. Methods Appl. Mech. Engrg.,* 190 (2000), pp. 1785-1800.
[26] G. Hauke, G. Sangalli, and M. H. Doweidar, Combining adjoint stabilized methods for the advection-diffusion-reaction problem, *Math. Models Methods Appl. Sci.,* 17 (2007), pp. 305-326.
[27] P.-W. Hsieh and S.-Y. Yang, A novel least-squares finite element method enriched with residual-free bubbles for solving convection-dominated problems, *SIAM J. Sci. Comput.,* 32 (2010), pp. 2047-2073.
[28] T. J. R. Hughes, Multiscale phenomena: Green's functions, the Dirichlet-to-Neumann formulation, subgrid scale models, bubbles and the origins of stabilized methods, *Comput. Methods Appl. Mech. Engrg.,* 127 (1995), pp. 387-401.
[29] T. J. R. Hughes, L. P. Franca, and G. M. Hulbert, A new finite element formulation for computational fluid dynamics: VIII. the Galerkin/least-squares method for advective-diffusive equations, *Comput. Methods Appl. Mech. Engrg.,* 73 (1989), pp. 173-189.
[30] G. R. Barrenechea and J. Blasco, Pressure stabilization of finite element approximations of time-dependent incompressible flow problems, *Comput. Methods Appl. Mech. Engrg.,* 197 (2007), pp. 219-231.
[31] T. Barth, P. Bochev, M. Gunzburger, and J. Shadid, A taxonomy of consistently stabilized finite element methods for the Stokes problem, *SIAM J. Sci. Comput.,* 25 (2004), pp. 1585-1607.
[32] L. P. Franca and S. L. Frey, Stabilized finite element methods: II. the incompressible Navier-Stokes equations, *Comput. Methods Appl. Mech. Engrg.,* 99 (1992), pp. 209-233.
[33] L. P. Franca and T. J. R. Hughes, Two classes of mixed finite element methods, *Comput. Methods Appl. Mech. Engrg.,* 69 (1988), pp. 89-129.
[34] M. A. Behr, *Stabilized Finite Element Methods for Incompressible Flows with Emphasis on Moving Boundaries and Interfaces,* Ph.D. thesis, Department of Aerospace Engineering and Mechanics, University of Minnesota, 1992.
[35] M. A. Behr, L. P. Franca, and T. E. Tezduyar, Stabilized finite element methods for the velocity-pressure-stress formulation of incompressible flows, *Comput. Methods Appl. Mech. Engrg.,* 104 (1993), pp. 31-48.
[36] M. A. Olshanskii and A. Reusken, Grad-div stabilization for Stokes equations, *Math. Comput.,* 73 (2003), pp. 1699-1718.
[37] G. R. Barrenechea and F. Valentin, Beyond pressure stabilization: A low-order local projection method for the Oseen equation, *Int. J. Numer. Meth. Engng.,* 86 (2011), pp. 801-815.
[38] P. G. Ciarlet, *The Finite Element Method for Elliptic Problems,* North-Holland Publishing Company, Amsterdam, 1987.
[39] H. C. Elman, D. J. Silvester, and A. J. Wathen, *Finite Elements and Fast Iterative Solvers: with Applications in Incompressible Fluid Dynamics,* Oxford University Press, New York, 2005.
[40] H.-Y. Duan, P.-W. Hsieh, R. C. E. Tan, and S.-Y. Yang, Analysis of a new stabilized finite element method for the reaction-convection-diffusion equations with a large reaction coefficient, *Comput. Methods Appl. Mech. Engrg.,* 247-248 (2012), pp. 15-36.
[41] I. Harari and T. J. R. Hughes, What are C and h?: Inequalities for the analysis and design of finite element methods, *Comput. Methods Appl. Mech. Engrg.,* 97 (1992), pp. 157-192.
[42] F. Hecht, O. Pironneau, J. Morice, A. Le Hyaric, and K. Ohtsuka, *FreeFem++, Third Edition, Version 3.19,* 2012, http://www.freefem.org/ff++/.